Anomalous transport and luminescence of indirect excitons in AlAs/GaAs coupled quantum wells as evidence for exciton condensation

L. V. Butov and A. I. Filin

Institute of Solid State Physics, Russian Academy of Sciences, 142432 Chernogolovka, Moscow district, Russia

Due to the long lifetime of indirect (interwell) excitons, exciton condensation (analogous to the Bose-Einstein condensation of bosons) is expected to occur in coupled quantum wells (CQW's). The critical conditions for the exciton condensation have been predicted to be strongly improved by high magnetic field perpendicular to the well plane. We present results of experimental study of transport and photoluminescence of indirect excitons in AlAs/GaAs CQW's at low temperatures ($T \geqslant 350$ mK) and high magnetic fields ($B \leqslant 14$ T). Strong anomalies in the transport and luminescence of indirect excitons have been observed at low temperatures and high magnetic fields: a large increase of the exciton diffusivity, a large increase of the exciton radiative decay rate and a huge noise in the integrated exciton PL intensity. An interpretation of the observed anomalies as evidence of the exciton condensation (i.e., in terms of the onset of exciton superfluidity, superradiance of the exciton condensate, and fluctuations near the phase transition) is analyzed. The parameter (temperature, exciton density, and magnetic field) dependences of the observed anomalous transport and photoluminescence of indirect excitons show that these effects are consistent with the exciton condensation in the presence of a random potential. [S0163-1829(98)04827-9]

I. INTRODUCTION: PROBLEM OF EXCITON CONDENSATION IN QUANTUM-WELL STRUCTURES

The electron-hole (e-h) interaction in a neutral e-h system can result in the condensation of bound e-h pairs (excitons) in a momentum space. In the case of a dilute exciton gas ($n a_B^d \ll 1$, where a_B is the exciton Bohr radius, n is the e-h density, and d is the dimensionality) the excitons can be considered as weakly interacting Bose particles, and the condensation is analogous to the Bose-Einstein condensation (BEC) of bosons,[1] while in the case of a dense e-h system ($n a_B^d \gg 1$) the excitons are analogous to Cooper pairs, and the exciton condensate, called the excitonic insulator, is analogous to the BCS superconductor state.[2] Contrary to the BCS superconductor state, the pairing in the excitonic insulator is due to e-h interaction; the pairs are neutral and the state is insulating. For exciton condensation in a dense e-h system, the nesting of electron and hole Fermi surfaces is required. The transition between the dilute and dense limits is smooth.[3]

The condensation conditions can be achieved only if the temperature of excitons is below a critical temperature T_c. For the condensation in a system of weakly interacting bosons, T_c is inversely proportional to the boson mass. As the effective exciton mass in semiconductors is small, of the order of the free-electron mass, T_c for exciton condensation is several orders of magnitude larger than T_c for the condensation of Bose atoms. The latter was recently observed experimentally with the critical temperature being in a (sub)-μK range.[4] For experimentally accessible exciton densities in semiconductors, T_c reaches several K. Nevertheless, in spite of the relatively high critical temperature, T_c is hard to achieve experimentally. Due to the e-h recombination, the exciton temperature can considerably exceed the lattice temperature. The exceeding of the exciton temperature over the lattice temperature is determined by the ratio between the exciton energy relaxation rate and the exciton recombination rate. Therefore, for searches of exciton condensation, semiconductors with a long exciton lifetime are selected in order to achieve low temperatures in the exciton system.

For observation of exciton condensation, semiconductors, in which the exciton condensate is the ground state, in particular, has a lower energy than metallic electron-hole liquid (which is a real space condensate) are required. The latter is the ground state in Ge and Si, and was intensively studied in the 1970s.[5]

Experimental efforts to observe exciton condensation in bulk semiconductors have concentrated mainly on studies of excitons in Cu_2O and in uniaxially strained Ge. These semiconductors are characterized by a long exciton lifetime and are, therefore, attractive for experimental searches of the exciton condensation. Degenerate Bose-Einstein statistics have been observed for excitons in Cu_2O (Ref. 6) and Ge.[7] Recently, overcoming of the exciton condensate phase boundary for paraexcitons[8] and ortoexcitons[9] in Cu_2O has been reported. The study of excitons in Cu_2O, with particular emphasis on the exciton condensation problem, is currently in progress.[10]

The semiconductor quantum-well (QW) structures provide an opportunity for experimental realization of a quasi-two-dimensional (2D) exciton condensate. Strictly speaking, for infinite 2D systems BEC, i.e., the macroscopic occupation of one (lowest energy) state with the number of particles in the state comparable with the total number of particles in the system, is possible only at $T=0$. At finite temperatures, only condensation into a superfluid state with the mean-field transition temperature $T_c \approx 4\pi\hbar^2 n / [2m \ln \ln(1/na^2)]$ is possible in the weakly interacting Bose gas in two dimensions (n is the density, m is the boson mass, and a is the range of interaction).[11,12] Below T_c the small momentum particles

contribute to a so-called quasicondensate, which results in the appearance of superfluidity.[11,12] Note that above the Kosterlitz-Thouless critical temperature, at $T_{KT} < T \lesssim T_c$, the superfluidity is local, and a macroscopic superfluid density abruptly appears at $T = T_{KT}$.[13] However, for a finite 2D system with an area S, the critical temperature for the BEC is nonzero: $T_{cS} = 2\pi\hbar^2 n/[m \ \ln(nS)]$,[14,15] and reduces logarithmically with the increase of the system area. Note that, for finite 2D systems, the energy spectrum is discrete (zero dimensional). The difference between the quasicondensate (macroscopic occupation of the low momentum/energy states) and the Bose-Einstein condensate (macroscopic occupation of one state) is not essential for most experiments;[11] therefore we will not distinguish between them when discussing exciton condensation in this paper.

In a general case of nonresonant excitation, the exciton condensate can be formed via the exciton energy relaxation toward the lowest-energy exciton state. In a sense of exciton energy relaxation, QW structures have certain advantages for the experimental realization of the exciton condensate as compared to 3D bulk systems. Below the optical-phonon energy, the energy relaxation of excitons is due to the acoustic phonons. In the region of subsonic wave vectors $k < ms/\hbar$ (s is the sound speed), the exciton relaxation on phonons diminishes sharply as a consequence of the impossibility to satisfy energy and momentum conservation laws simultaneously. This results in the impossibility of exciton condensation by means of phonon cooling only if the exciton lifetime is not very long, > ms.[16,17] The reduction of the exciton energy relaxation rate in the region of subsonic wave vectors was shown to be strongly weakened for 2D exciton–3D phonon systems due to momentum nonconservation in the z direction, which allows the energy relaxation of subsonic excitons via consequent absorption and emission of acoustic phonons; in particular, the 2D exciton condensation time was calculated to be in the range of nanoseconds which is several orders of magnitude shorter than the 3D exciton condensation time.[18] Also, during exciton energy relaxation with optical- and/or acoustic-phonon emission, phonons escape out of the QW plane into the bulk, which results in more effective cooling both of the lattice around the QW and of the QW exciton system compared to the homogeneously excited bulk systems.

It was shown by Lerner and Lozovik and Kuramoto and Horie that critical conditions for exciton condensation in QW's can be drastically improved by a high magnetic field perpendicular to the well plane.[19,20] At zero magnetic field in the dense e-h system, T_c is determined by dissociation of the condensed pairs; conversely, dissociation is negligible in the dilute limit, and only the exciton center of mass excitations are relevant: T_c is reached when the $k = 0$ state is empty. In high magnetic fields the internal structure of the exciton and its center-of-mass motion are coupled:[21] the average in-plane spatial separation between the electron and hole is proportional to the exciton center-of-mass momentum. Therefore, the emptying of $k = 0$ states is accompanied by exciton dissociation (in this sense, even in the limit of low exciton density the condensate of magnetoexcitons resembles the excitonic insulator). The coupling results in a strong modification of the density dependence of T_c. In the high-magnetic-field limit, the mean-field critical temperature for the
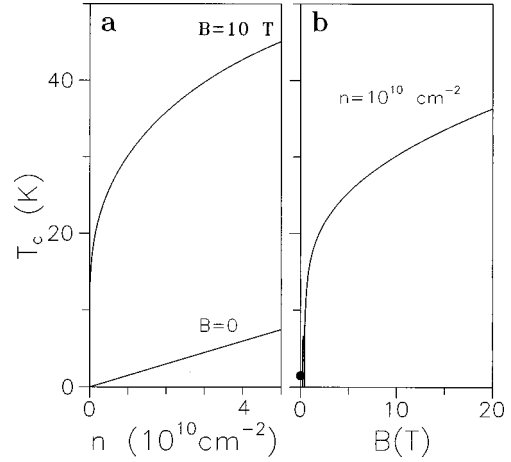

FIG. 1. Comparison of the theoretically predicted critical temperature for the condensation of two-dimensional excitons, T_c, at $B = 0$ and at high magnetic field ($B = 10$ T) vs exciton density (a). At $B = 0$, the critical temperature is presented by $T_{c0} = 2\pi\hbar^2 n/m$ for $m = 0.37 m_0$, which refers to the indirect exciton mass in AlAs/GaAs CQW's (the logarithmic corrections are omitted, see text). In high magnetic fields the critical temperature is presented by the LL-KH formula $T_{cB} = E_B(1 - 2\nu)/[2 \ \ln(\nu^{-1} - 1)]$ (Refs. 19 and 20); see text. The predicted magnetic-field dependence of T_c at $n = 10^{10}$ cm^{-2} is presented by the LL-KH formula (b); see text. The point at $B = 0$ presents $T_{c0}(B = 0)$. The spin degeneracy is neglected in the dependences.

condensation of two-dimensional excitons was calculated to be $T_{cB} = E_B(1 - 2\nu)/[2 \ \ln(\nu^{-1} - 1)]$ for $0 \le \nu \le 1$, where $E_B = \sqrt{\pi/2} e^2/(\epsilon_0 l_B)$ is the magnetoexciton binding energy, $\nu = n/n_L$ is the Landau-level filling factor, ϵ_0 is the dielectric constant, and $l_B = \sqrt{\hbar c/eB}$ is a magnetic length.[19,20,22] At low densities, T_{cB} is much higher than the zero-field critical temperature, which has a roughly linear density dependence (see above). The comparison of the predicted critical temperature for exciton condensation at zero and high magnetic fields is shown in Fig. 1 for the parameters relevant to our experiments described below. For an estimate, the critical temperature at $B = 0$ is presented by $T_{c0} = 2\pi\hbar^2 n/m$ for $m = 0.37 m_0$ which refers to the indirect exciton mass in AlAs/GaAs coupled QW's studied in this paper. The logarithmic corrections are omitted, therefore, T_{c0} is higher than T_c (Refs. 11 and 12) and T_{cS}.[14,15] The critical temperature at high magnetic field, T_{cB}, is presented by the formula of Lerner-Lozovik and Kuramoto-Horie (LL-KH). It should be noted that the LL-KH theory was developed for the high-magnetic-field limit, where the electron and hole cyclotron energies are much larger than E_B. Its predictions for $B = 10$ T and smaller fields can be considered qualitatively only. In particular, the infinite derivative of $T_{cB}(n)$ at $n = 0$ [Fig. 1(a)] is the artifact of the high-magnetic-field approximation, for a finite field the derivative should be finite. Similarly, the strong increase of $T_{cB}(B)$ at small B [Fig. 1(b)] is overestimated in the high-magnetic-field approximation; the oscillations at small fields corresponding to $\nu > 1$ are also the artifact of the high-magnetic-field approximation. Still, qualitatively, the LL-KH theory implies a strong increase of T_c at high magnetic fields compared to $B = 0$ case (Fig. 1). Note that the magnetic-field dependence of T_{KT} is the opposite: T_{KT} is reduced with increasing B mainly due to the
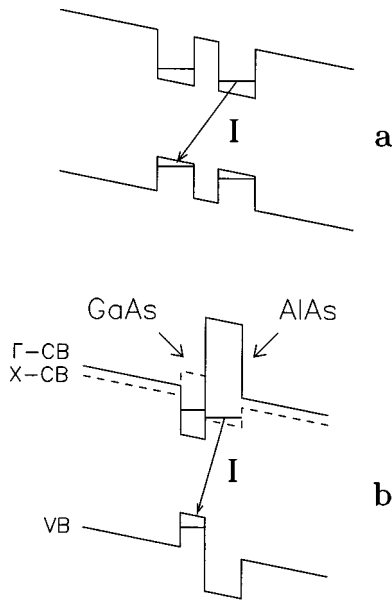
FIG. 2. Schematic band diagram of a-type CQW's (a) and b-type AlAs/GaAs CQW's (b) in the indirect regime. The indirect transitions are indicated by the arrows.

increase of the magnetoexciton mass.[19] A theory of the exciton condensation in finite magnetic fields has not yet been developed at present.

In addition, the magnetic field lifts off the spin degeneracy of the exciton state, which also results in an increase of the critical temperature for the exciton condensation due to the effective increase of n; in all equations for the critical temperatures above, n/g should be used instead of n for the state degeneracy $g \neq 1$.

The predictions of LL-KH theory have initiated experimental searches of the 2D exciton condensation in high magnetic fields. The precursor of the exciton condensation in QW's at high magnetic fields, namely, the formation of excitons in a dense 2D e-h system, has been observed in $In_xGa_{1-x}As/InP$ QW's (these QW's are characterized by a relatively low temperature of the photoexcited carriers compared to $In_xGa_{1-x}As/GaAs$ and $GaAs/Al_xGa_{1-x}As$ QW's).[23] However, due to the relatively short exciton lifetime in the single QW's studied and, hence, the high exciton temperature, the exciton condensation phase boundary was not overcome.

The e-h recombination rate is strongly reduced in coupled QW's (CQW's), where electrons and holes are confined in different QW's. Due to the long recombination lifetime of indirect (interwell) excitons, CQW's are considered as good candidates for the observation of 2D exciton condensation.[20,24–27] The examples of semiconductor CQW types are shown in Fig. 2. In a-type CQW's [Fig. 2(a)], electrons and holes are spatially separated by a potential barrier which provides the small overlap of electron and hole wave functions resulting in the long recombination lifetime of indirect excitons. Different materials can be chosen for the well-barrier combination in a-type CQW's: typical examples are the GaAs well–$Al_xGa_{1-x}As$ barrier, and $In_xGa_{1-x}As$ well–GaAs barrier. In b-type CQW's [Fig. 2(b)], the effective spatial separation between electrons and holes is small

compared to a-type CQW's. The electron state in AlAs is constructed from the X minima of the conduction band. Together with the spatial separation between electrons and holes in the z direction, this results in the long lifetime of indirect excitons in b-type CQW's. Both in a- and b-type CQW's, the exciton lifetime can be controlled by the electric field in the z direction, which is determined by an external gate voltage.[28,29]

An unavoidable property of semiconductor QW's and CQW's is the existence of a random potential in the well plane induced by the interface and alloy fluctuations, defects and impurities. The random potential strongly influences the properties of the exciton condensate in QW's. Note, e.g., that, even for infinite 2D systems, disorder results in the in-plane confinement of bosons, which allows BEC at nonzero temperatures in analogy to the BEC in finite 2D systems. The problem of (2D) boson condensation in a disordered medium was studied theoretically[30–34] mainly in connection with the superfluidity of liquid ^{4}He in porous media or on substrates[35] and superconductivity in granular[36] and uniformly disordered superconductor films.[37–39] In particular, the boson localization and the superfluid-insulator transition were studied. A qualitative behavior of the exciton condensate in the random potential is supposed to be the following. For zero potential fluctuations the exciton condensate is homogeneous in space, and spreads over the sample for the net repulsive interaction between excitons, which was calculated to be the case for indirect excitons in CQW's.[27,40] For nonzero potential fluctuations a random array of the normal areas and the exciton condensate lakes (domains), with boundaries determined by the potential profile, is formed. This state is analogous to the ''Bose-glass'' phase considered in Ref. 31. With the increase of the potential fluctuations the sizes of the condensate lakes (as well as the phase correlation between the lakes) are reduced, and at large random potential the exciton condensate disappears. The ultimately large disorder can result in the breaking of excitons, and in separate localization of electrons and holes in different potential minima. Therefore, in order to observe the exciton condensate, samples with small potential fluctuations are required.

Below, we discuss the expected specific properties of the exciton condensate which can be detected in exciton luminescence and transport experiments. The condensation of long-life interacting indirect excitons in CQW's should be accompanied by the appearance of exciton superfluidity.[20,24,25] The interaction results in a linear dispersion of the collective modes in the exciton system and, consequently, in fulfillment of the Landau criterion of superfluidity,[19,20,24,25,41] while the long lifetime of indirect excitons removes the problem of the order parameter phase fixation.[24] The latter problem was pointed out by Guseinov and Keldysh,[42] and is in the following: interband transitions (e-h recombination) fix the phase of the exciton condensate order parameter, which makes impossible a superfluid state with a uniform particle flow. The highest interband transition rate at which the exciton superfluidity is still possible was calculated in Ref. 43.

The exciton condensation should be accompanied by the change of the exciton optical properties. As the photoluminescence (PL) line shape reflects the distribution of excitons over the exciton states (with a weight proportional to the

radiative recombination probability of the state), exciton condensation in homogeneous media should result in the narrowing of the exciton PL line and in the appearance of a sharp PL peak corresponding to the emission of the macroscopically occupied state. Just such an appearance of a sharp peak in the exciton PL spectra was reported in Refs. 8 and 9 as evidence of exciton condensation in Cu_2O. However, the spatially integrated PL line shape of excitons in QWs (or CQW's) is mainly determined by the random potential, and reflects the distribution of excitons over a huge number of local potential minima; therefore, a spatially integrated PL line shape can hardly be used for an analysis of exciton condensation in QW's.[44,45]

Exciton condensation is expected to be accompanied by exciton condensate superradiance, which can be detected as a strong increase of the exciton radiative decay rate. In spite of the absence of a detailed theoretical treatment of this effect, indications of such behavior can be found in Ref. 46, where the divergence of the exciton radiative decay rate was obtained when approaching T_c from above. The increase of the exciton radiative decay rate at the exciton condensation can be understood in the following terms. Only 2D excitons with small momenta $k \leq k_0 \approx E_g \sqrt{\epsilon}/\hbar c$ can decay radiatively (where E_g is the gap, ϵ is the high-frequency dielectric constant, and c is the light speed). The oscillator strength of the optically active 2D excitons is increased with the increase of the lateral size of the exciton center-of-mass wave function, called the exciton coherent area, and saturates when the coherence length reaches the inverse wave vector of the emitted light[47–52] (the origin of this effect is similar to the giant exciton oscillator strength first proposed by Rashba and Gurgenishvili[53]). For normal uncondensed excitons, the coherent area is determined by the exciton localization length and the exciton scattering length.[47–52] For condensed excitons, the whole size of the condensate is the coherent area which implies a large exciton oscillator strength. A macroscopic mechanism for the increase of the exciton coherence area at the exciton condensation in the presence of a random potential is not trivial, and requires theoretical consideration. Intuitively, it follows from an increase of the exciton-exciton and exciton-phonon scattering lengths at the exciton condensation, as well as from a presumable increase of the exciton localization length due to the enhanced exciton screening of the random potential at the condensation,[54] and due to a settling of the phase coherence among the condensate lakes (the latter effect was briefly discussed in Ref. 32). In addition, at the exciton condensation the measured radiative exciton decay rate is increased due to an increase of the fraction of the optically active excitons with $k \leq k_0$. The energy of the optically active excitons $\leq E_0 = \hbar^2 k_0^2 / 2m \approx 0.8$ K, which refers to the AlAs/GaAs heavy-hole indirect exciton mass $m = 0.37 m_0$ [for the X_z heavy-hole indirect exciton in AlAs/GaAs CQW's, $m_e = 0.19 m_0$, while the literature data for m_h scatter; we use the value $m_h = 0.18 m_0$ (see Ref. 55 and references therein), and $m = m_e + m_h = 0.37 m_0$ for the estimates in this paper]. The measured radiative decay rate is proportional to the fraction of excitons with $k \leq k_0$, which is equal to $1 - \exp(-E_0 / k_B T)$ for the Boltzmann distribution; for $T \gg E_0$, Boltzmann distribution results in the linear increase of the exciton radiative decay time with temperature.[47–51] Exciton condensation is characterized by the macroscopic occu-

pation of the lowest-energy state which, together with the increase of the exciton oscillator strength, should result in an increase of the exciton radiative decay rate at the exciton condensation.

We have performed an experimental study of the transport and luminescence of indirect excitons in AlAs/GaAs CQW's [Fig. 2(b)] at high magnetic fields ($B \leq 14$ T) and low bath temperatures ($T_{bath} \geq 350$ mK). The lifetime of indirect excitons in the structure was long enough for exciton thermalization down to temperatures of the order of 1 K. Following the predictions of Lerner-Lozovik and Kuramoto-Horie (see Fig. 1), a high magnetic field perpendicular to the CQW plane was applied in order to improve the critical conditions for exciton condensation. The b-type CQWs considered have advantages for the exploration of exciton condensation in high magnetic fields compared to what is possible with a-type CQW's. It has been shown[40,56] that for $d \leq l_B$ (d is the effective distance between the electron and hole layers) the ground state is determined by e-h interaction and is the exciton condensate at low temperatures, while for $d \geq l_B$ the ground state is determined by e-e and h-h interaction and the exciton condensate is not stable (in the limit of low random potential, the ground state was predicted to be the coupled electron and hole Laughlin liquids or the coupled electron and hole Wigner solids[40,56]). At $B = 10$ T, $l_B = 8.1$ nm. Therefore, a high magnetic field of the order of 10 T should destroy the exciton condensate in a-type CQW's, which typically have $d \geq 10$ nm, and, conversely, should improve critical conditions for exciton condensation in b-type CQW's which have $d \approx (3-4)$ nm. The small e-h separation is also important because the calculated critical temperature for exciton condensation in high magnetic fields is proportional to the magnetoexciton binding energy (see above). The possibility of exciton condensation in the studied AlAs/GaAs CQW's is analyzed by a comparison of the experimental data with the expected properties of the exciton condensate.

The paper is organized as follows: The CQW sample design, the experimental setup, and the CQW PL characterization spectra at $B = 0$ are presented in Sec. II. The indirect exciton PL decay, transport, and radiative decay rate are considered in Sec. III. The variations of the indirect exciton PL decay with the gate voltage and, in particular, a strongly indirect regime are considered in Sec. IV. The fluctuations of the indirect exciton PL intensity are considered in Sec. V, followed by conclusions in Sec. VI. Finally, in the Apendixes, we consider the influence of the nonexponentiality of the PL decay on the exciton radiative decay rate derivation, the relation between the indirect exciton transport and the direct excitons in natural quantum dot emission, and the influence of the sample degradation on the observed effects.

II. SAMPLES AND EXPERIMENTAL SETUP

The studied electric field tunable n^+-i-n^+ AlAs/GaAs CQW structures have been grown by molecular-beam epitaxy. The i region consists of a 4-nm AlAs layer and a 3-nm GaAs layer, surrounded by two 40-nm $Al_{0.48}Ga_{0.52}As$ barrier layers (followed by 5-nm GaAs layers) (Fig. 1). The n^+ layers are Si-doped GaAs with $N_{Si} = 2 \times 10^{18}$ cm^{-2}. Due to the metallic character of the n^+ layers, the external gate voltage V_g, applied between the front gate on the mesa top

and the back gate on the bottom of the n^+ substrate, drops entirely in the i region. The front gate is designed as the gold frame around the mesa structure with a 200×200-μm^2 window.[29] The lateral homogeneity of the electric field in the structure is provided by the metallic character of the n^+ layers. In the direct regime ($V_g \gtrsim 0.4$ V for the CQW's studied), both electrons and holes are confined in the GaAs QW. In the indirect regime ($V_g \lesssim 0.4$ V), electrons are in the AlAs QW and holes in the GaAs QW. The ground electron state in AlAs in the studied 4-nm AlAs–3-nm GaAs CQW's is constructed from the X_z minima of the conduction band and is twofold degenerate, the fourfold degenerate electron state constructed from the X_{xy} valleys of the conduction band is about 40 meV higher in energy.[29]

As the electron Fermi level in the n^+ GaAs layers is well below the electron energies in the GaAs and AlAs QW's, the QWs are nominally empty in the absence of photoexcitation (the concentration of the residual impurities in the QW region is unknown; however, it is well below the Mott density to provide free electron or hole gases in the QW's, and below the density of photoexcited excitons in the CQW's studied). Carriers were photoexcited in the GaAs QW, with the photon energy below the $Al_{0.48}Ga_{0.52}As$ barriers, by either a cw dye laser ($\hbar\omega=1.85$ eV) or a pulsed semiconductor laser ($\hbar\omega=1.8$ eV, the pulse duration is 30 or 50 ns, and the edge sharpness including the system resolution is 0.7 ns). The sub-barrier photoexcitation eliminates the problem of carrier collection into the QW's, as well as the problem of variation of the electric field in the structure caused by the carrier accumulation in layers other than the AlAs and GaAs QW's.[57,58]

Excitation and detection of the PL signal were performed by means of an optical fiber with a diameter of 100 μm positioned approximately 300 μm above the mesa. In order to minimize the effect of the mesa heating, the total sample area of about 1 mm^2 was much larger than the mesa size, and the bottom of the sample was soldered to the metal plate. Measurements were performed in a liquid or vapor ^{3}He (350 mK$\leq T \leq$10 K), as well as in a liquid or vapor ^{4}He (1.3$\leq T \leq$10 K). The sample temperature was measured by the coil resistance soldered on the same metal plate as the sample, approximately 1 mm from the sample (this design minimizes the difference between the sample temperature and the measured temperature). The PL signal was dispersed by a double-grating monochromator and detected by a Si-avalanche diode or a photomultiplier. Time-resolved experiments were performed by means of a time-correlated photon counting system, while in cw experiments a charge coupled device (CCD) camera or a photon-counting system or lock-in amplifier were used.

The characterization zero-magnetic-field PL spectra in the indirect regime at cw excitation with $W_{ex}=50$ and 500 W/cm^2 are shown in Fig. 3. At high excitations the indirect PL line broadens, indicating the appearance of e-h plasma; in addition, the temperature of the system is increased, which results in the appearance of a PL line of direct excitons. An increase of indirect exciton density was found to result in a monotonic increase of the indirect PL energy. This behavior corresponds to the theoretically predicted increase of the indirect exciton energy with density,[27,40] and can be understood in terms of the net repulsive interaction between indi-
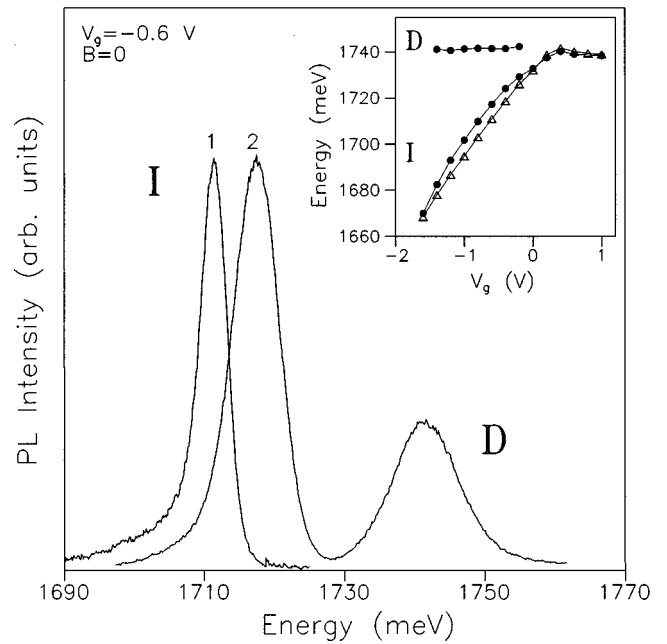

FIG. 3. Normalized PL spectra of the AlAs/GaAs CQW (sample $S1$) in the indirect regime ($V_g = -0.6$ V) at cw excitation with excitation densities $W_{ex}=50$ (1) and 500 W/cm^2 (2); $T=350$ mK. Inset: V_g dependence of the direct (D) and indirect (I) transitions at $T=350$ mK for $W_{ex}=50$ (triangles) and 500 W/cm^2 (points).

rect excitons caused by the dipole-dipole repulsion for low exciton densities, and in terms of the energy shift originated from the electric field between the separated electron and hole layers for high e-h densities. The observed monotonic increase of the indirect exciton energy with density implies that the exciton state is the ground state in the system, in particular, has lower energy than metallic electron-hole liquid. This corresponds to the theoretical predictions for a spatially separated system of electrons and holes.[27,40]

The direct and indirect exciton transition energies are shown in the inset to Fig. 3 as a function of V_g for different excitation densities. In the indirect regime the shift of the indirect exciton energy with V_g is almost linear at low exciton densities, and corresponds to the CQW potential profile variation by V_g. For the fixed V_g the magnitude of the indirect exciton energy shift with W_{ex} is determined by the indirect exciton density. Therefore, as a function of V_g the maximum indirect exciton energy shift for fixed W_{ex} (see the inset to Fig. 3) corresponds to the maximum exciton density which is determined by the maximum exciton lifetime. Close to the direct regime the exciton lifetime is reduced due to the Γ-X mixing,[29] while at $V_g \lesssim -1$ V it is reduced by tunneling of carriers through the $Al_xGa_{1-x}As$ barriers. The maximum indirect exciton energy shift corresponding to the maximum exciton lifetime in the structure is observed around $V_g = -0.8$ V (inset to Fig. 3).

III. PL DECAY, TRANSPORT, AND RADIATIVE DECAY RATE OF INDIRECT EXCITONS IN HIGH MAGNETIC FIELDS

The indirect regime at $V_g = 0$ is considered in this section. We start from an analysis of the PL decay of indirect exci-
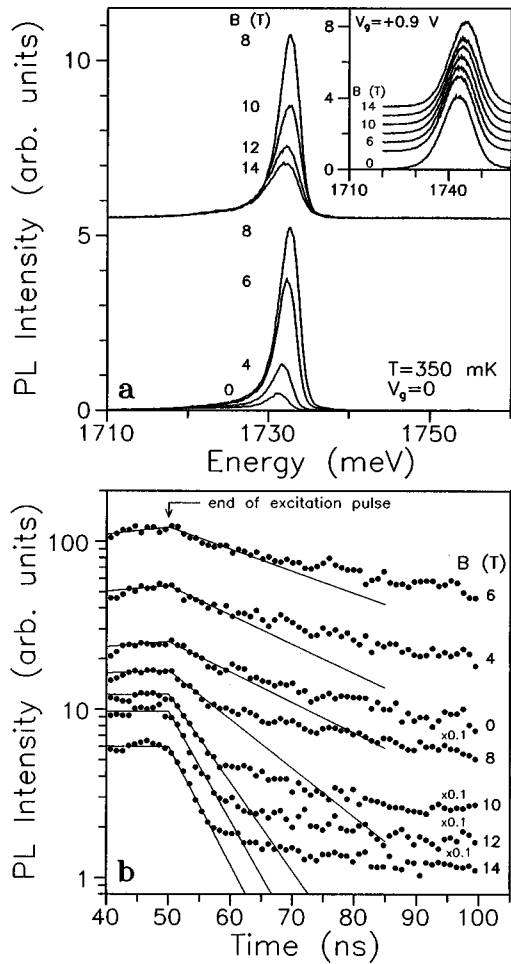
FIG. 4. Magnetic-field dependence of the time-integrated PL spectrum (a) and the PL decay (b) of indirect excitons in the AlAs/ GaAs CQW (sample $S2$) in the indirect regime ($V_g = 0$) at $T = 350$ mK and $W_{ex} = 10$ W/cm^2 (pulse duration 50 ns). Thin lines are the fitting curves for the initial times of the PL decay. Inset: magnetic-field dependence of the time-integrated PL spectrum of direct excitons in the AlAs/GaAs CQW in the direct regime ($V_g = +0.9$ V) at the same excitation and temperature.

tons in high magnetic fields. The first data on the indirect exciton PL decay in high magnetic fields were reported in Ref. 59. The magnetic field was found to result in a strong variation both of the time-integrated indirect exciton PL intensity and the indirect exciton PL decay. Figure 4 shows the time-integrated indirect exciton PL spectra as well as the PL decay curves at $T = 350$ mK at a fixed photoexcitation ($W_{ex} = 10$ W/cm^2, excitation pulse duration 50 ns) versus magnetic field. For comparison, the direct exciton PL spectra in the direct regime ($V_g = +0.9$ V) at the same photoexcitation are shown in the inset. The PL decay curves were recorded with spectrum integration within a 3-meV spectral range centered at the maximum of the indirect exciton PL line. There is a clear difference of the indirect exciton PL intensity decay. At $B \lesssim 6$ T the decay is slightly nonexponential with a relatively long time constant. At higher magnetic fields a rapid initial decay is followed by a slow decay at larger times [Fig. 4(b)]. The indirect exciton PL intensity is first increased with an increase of B (at $B \lesssim 8$ T), and then reduced [Fig. 4(a)]. Conversely, the direct exciton PL inten-

sity in the direct regime is almost independent of B (inset to Fig. 4).

Note that the PL linewidth of the direct exciton (about 11 meV) is larger than the PL linewidth of the indirect exciton (about 3 meV); see Fig. 4(a). The perpendicular electron effective mass for the indirect exciton ($1.1m_0$) is much larger than that for direct exciton ($0.077m_0$) and, therefore, the interface fluctuations (which are the main origin of the disorder for 2D excitons in the considered narrow CQW structure) result in much smaller variations of the indirect exciton energy compared to the direct exciton energy.[29] Note also that the fluctuations of the internal interface, between the GaAs and AlAs layers, are effectively cancelled for indirect excitons, as their influence on the electron and hole energy have opposite sign.[55] Effectively, the interface fluctuations produce a smaller disorder for indirect excitons compared to direct excitons in AlAs/GaAs CQW's.

No direct exciton PL is observed in the indirect regime for $W_{ex} = 10$ W/cm^2 [Fig. 4(a)]. Therefore, the direct exciton density is negligibly small in the indirect regime (the ratio between the direct and indirect exciton densities in the indirect regime is proportional to the ratio between the direct and indirect PL line intensities multiplied by the ratio between the direct and indirect exciton radiative decay times).

The integrated PL intensity of indirect excitons normalized to the integrated PL intensity in the direct regime, I_{PL}/I_D, as well as the initial PL decay time, τ, for $T = 350$ mK are plotted versus magnetic field in Figs. 9(c) and 9(e), see below. To disregard the indirect PL line low-energy tail emission corresponding to strongly localized excitons,[60] the spectral integration for I_{PL} was done within a 3-meV spectral range centered in the maximum of the indirect exciton PL line; the difference in the indirect and direct exciton PL linewidths was included in the ratio of integrated PL intensities, I_{PL}/I_D. In the indirect regime the integrated PL intensity is much smaller as compared to the direct regime [Fig. 9(c)], which means that the quantum efficiency is much smaller than unity. Therefore, for the studied CQW's in the indirect regime, the radiative lifetime τ_r is much larger than the nonradiative lifetime τ_{nr}, and the measured PL decay time $\tau \approx \tau_{nr}$.

Direct measurements of the exciton transport in AlAs/ GaAs CQW's by spatially resolved imaging of the exciton cloud extension performed simultaneously with the PL decay measurements, have shown that τ ($\approx \tau_{nr}$) is mainly determined by exciton transport to nonradiative recombination centers (NC's), and is reduced (increased) with the increase (reduction) of the exciton diffusivity.[61] This conclusion is typical of narrow QW structures characterized by relatively large random potentials induced by the interface fluctuations and, hence, small exciton diffusivities: for the narrow QW's the exciton transport time to NC's is large compared to the NC capture/recombination time and, therefore, determines τ_{nr}.[62] The similar relation between the measured indirect exciton PL decay time and indirect exciton transport in AlAs/GaAs CQW's was argued in Refs. 63 and 64. Therefore, the variations of τ in our CQW's may reflect changes in the exciton transport. Under this assumption, the observed magnetic-field dependence of τ implies that the increase of B first leads to a small reduction of the exciton diffusivity and then to a strong increase [Fig. 9(e)].
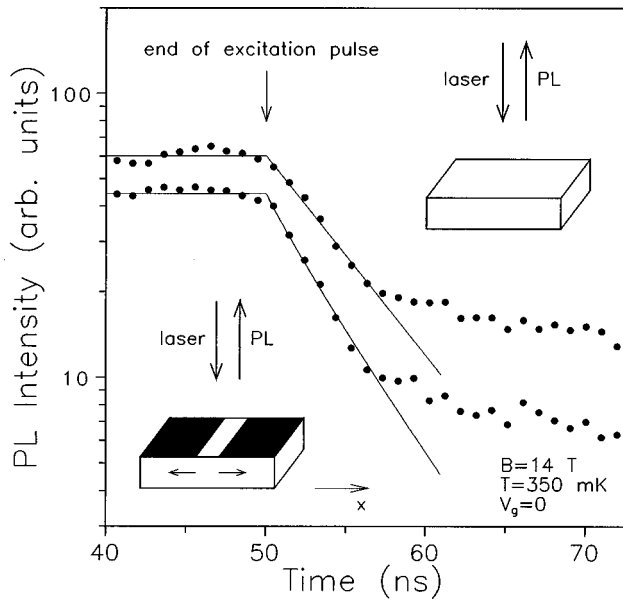
FIG. 5. Scheme of the exciton transport measurements by the time-of-flight technique. The curves present the indirect exciton PL decay in the AlAs/GaAs CQW (sample $S2$) for the unmasked (upper curve) and masked parts of the sample at $T = 350$ mK, $B = 14$ T, $V_g = 0$, and $W_{ex} = 10$ W/cm^2 (pulse duration 50 ns). The curves are shifted in the vertical axis for clarity. The difference between the decay rates is due to the exciton diffusion underneath the nontransparent regions of the mask shown by arrows on the lower scheme. Thin lines are the fitting curves for the initial times of the PL decay.

For direct measurements of the exciton transport, we have used a time-of-flight technique: the PL decay from an unmasked part of the sample was compared with the PL decay from a part of the sample which was covered by a nontransparent NiCr mask, leaving an array of 4-μm-wide stripes uncovered and separated from each other by 32 μm. Excitation and detection of the PL signal were performed by means of an optical fiber with a diameter of 100 μm positioned in front of either the masked or unmasked part of the sample. A similar time-of-flight technique (with different mask configuration) was used for a study of the direct exciton transport in GaAs/Al$_x$Ga$_{1-x}$As QW's.[65] The first data on indirect exciton diffusivity in high magnetic fields measured by the time-of-flight technique were reported in Ref. 66.

For the PL decay in the masked part of the sample, due to diffusion of excitons underneath the metal-covered regions, the variation of the exciton density is described by $\partial n/\partial t = G + D\partial^2 n/\partial x^2 - n/\tau$ during the photoexcitation, and by $\partial n/\partial t = D\partial^2 n/\partial x^2 - n/\tau$ after the end of the excitation pulse, where G is the generation rate and D is the exciton diffusion coefficient describing the exciton transport at the initial times of the PL decay (the validity of the description of exciton transport by the one-component diffusion equation with a single diffusion coefficient is discussed below). The measured PL intensity for the masked part of the sample, $I_{PL}^{masked}(t)$, is proportional to the exciton density integrated over the window regions. For the PL decay in the unmasked part of the sample, the term $D\partial^2 n/\partial x^2$ was neglected due to the large size of the excitation spot. Therefore, the PL decay for the masked part of the sample is more rapid compared to that for the unmasked part, due to the exciton diffusion out
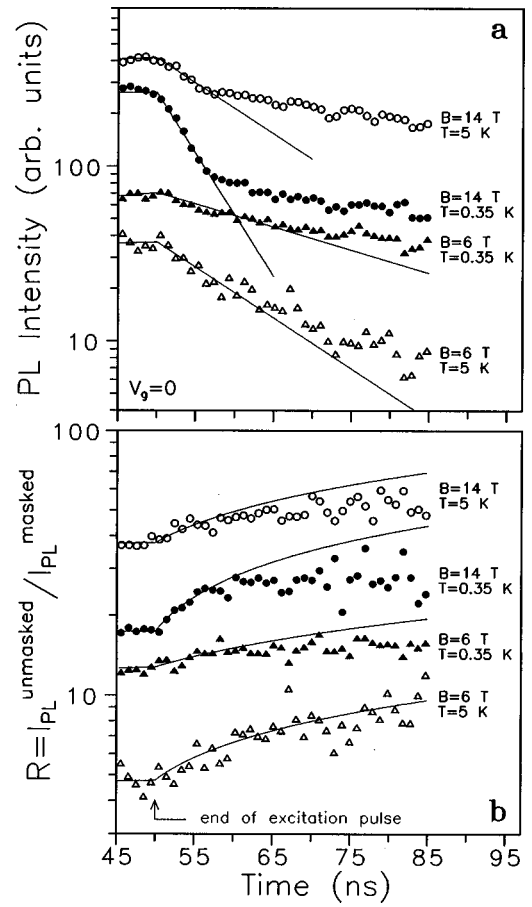

FIG. 6. Comparison between the indirect exciton PL decay in the AlAs/GaAs CQW (sample $S2$) (a) and the time dependence of the ratio between the indirect exciton PL intensities from the unmasked and masked parts of the sample (b) at $V_g = 0$ and $W_{ex} = 10$ W/cm^2 (pulse duration 50 ns), for low and high temperatures (0.35 and 5 K), and for low and high magnetic fields (6 and 14 T). The curves are shifted in the vertical axis for clarity. Thin lines are the fitting curves for the initial times of the PL decay.

of the window regions. An example of the PL decay for the masked and unmasked parts of the sample is shown in Fig. 5. We believe that the covering of the sample surface by the nontransparent metal mask does not change τ_{nr} (and hence τ as $\tau \approx \tau_{nr}$) underneath the metal-covered regions because of the large distance between the CQW and the sample surface (150 nm), and because the metal film is covered above another metal layer—n^+ GaAs. We also believe that possible reabsorption induced by the metal mask underneath the metal-covered regions is negligible due to the small absorption coefficient of indirect excitons.

The difference in the PL decays for the unmasked and masked parts of the sample can be presented by the time evolution of the ratio between the PL intensities, $R(t) = I_{PL}^{unmasked}(t)/I_{PL}^{masked}(t)$. The characteristic examples of $R(t)$ for low and high temperatures, and for low and high magnetic fields, are shown in Fig. 6(b). The constant value of $R(t)$ during the PL decay implies that the exciton diffusion underneath the metal-covered regions in the masked part of the sample is absent. The higher D is, the more strongly $R(t)$ deviates from the constant. Figure 6(b) shows that the deviation of $R(t)$ from the constant is strongest at the beginning of
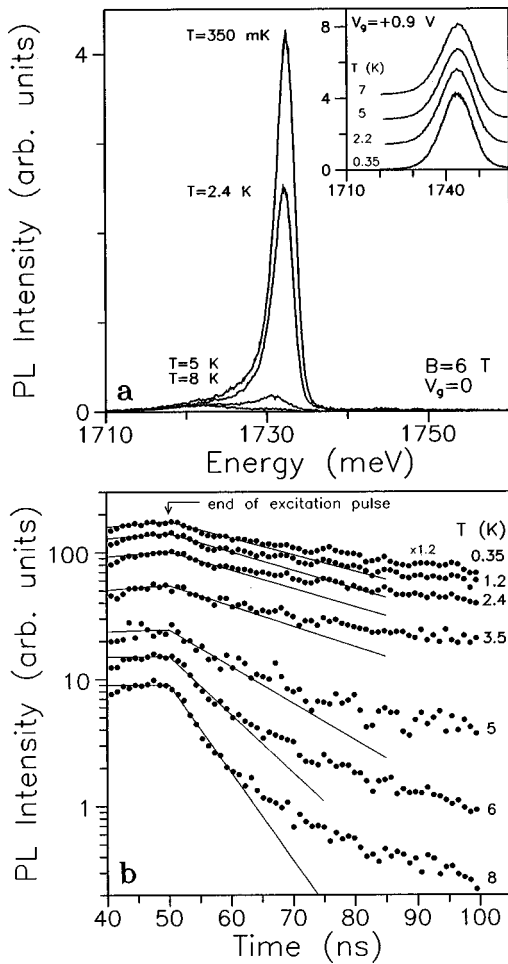
FIG. 7. Temperature dependence of the time-integrated PL spectrum (a) and the PL decay (b) of indirect excitons in the AlAs/GaAs CQW (sample $S2$) in the indirect regime ($V_g=0$) at $B=6$ T and $W_{ex}=10$ W/cm^2 (pulse duration 50 ns). Thin lines are the fitting curves for the initial times of the PL decay. Inset: temperature dependence of the time-integrated PL spectrum of direct excitons in the AlAs/GaAs CQW in the direct regime ($V_g=+0.9$ V) at the same excitation and magnetic field.
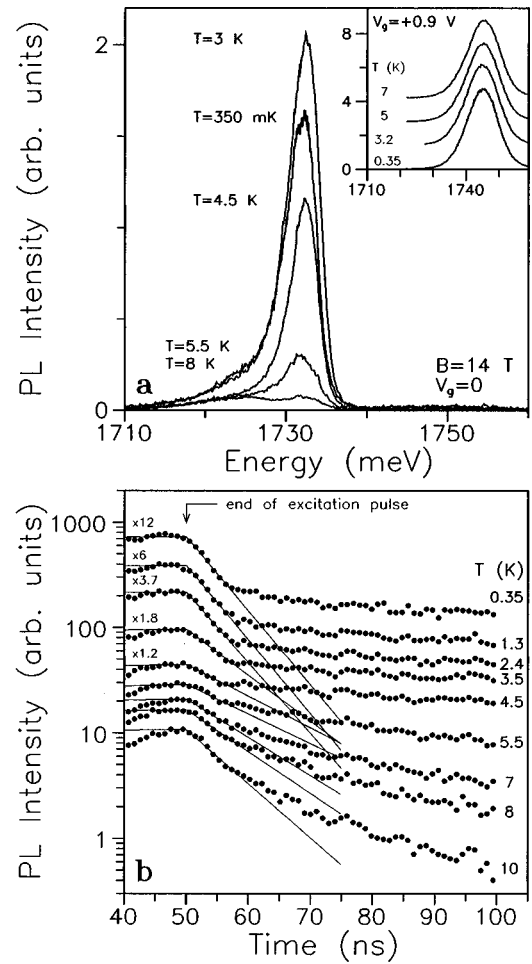
FIG. 8. Temperature dependence of the time-integrated PL spectrum (a) and the PL decay (b) of indirect excitons in the AlAs/GaAs CQW (sample $S2$) in the indirect regime ($V_g=0$) at $B=14$ T and $W_{ex}=10$ W/cm^2 (pulse duration 50 ns). Thin lines are the fitting curves for the initial times of the PL decay. Inset: temperature dependence of the time-integrated PL spectrum of direct excitons in the AlAs/GaAs CQW in the direct regime ($V_g=+0.9$ V) at the same excitation and magnetic field.

the PL decay, and reduces with delay time during the decay (for all temperatures and magnetic fields). The thin lines in Fig. 6(b) are the fitting curves for the initial times of the PL decay which use D as a fitting parameter; τ is determined separately from the PL decay for the unmasked sample.

The magnetic-field dependence of D at $T=350$ mK is shown in Fig. 9(g). D first slightly decreases with increasing magnetic field (this decrease is within the error bars), and then strongly increases. The temperature dependence of the integrated exciton PL intensity, τ and D for $B=6$ and 14 T, is shown in Figs. 9(d), 9(f), and 9(h). The data for $B=6$ T represent typical variations of τ and D at low magnetic fields, while the data for $B=14$ T are characteristic of high fields where rapid exciton transport is observed at low temperatures. The corresponding temperature dependences of the indirect exciton PL spectrum and the PL decay are shown in Figs. 7 and 8. Temperature dependences for $B=0$ are also presented in Fig. 9. Figure 9 shows that at $B=6$ T an increase of temperature results in an increase of D and a reduction of τ. Contrary to this, at $B=14$ T an increase of

temperature results in a reduction of D and an increase of τ at $T \lesssim 5$ K. Only at higher temperatures does τ start to drop, approaching the behavior observed for low magnetic fields. In all experiments an increase (reduction) of τ corresponds to a reduction (increase) of D. This confirms the assumption that τ is determined by exciton transport to nonradiative recombination centers. The relation between τ and D also persists with an increase of delay time: the differential decay time increases with delay time [Fig. 6(a)]. This is consistent with the reduction of the exciton diffusion coefficient with delay time, which is seen as the reduction of the deviation of $R(t)$ from the constant [Fig. 6(b)].

The observed variations of the exciton diffusion coefficient, and corresponding variation of the nonradiative lifetime with temperature and magnetic field, are discussed below. At low magnetic fields ($B \lesssim 6$ T), the temperature and magnetic-field dependences of τ and D [Figs. 9(e)–9(h)] are typical of thermally activated exciton transport in a random potential. The increase of the exciton diffusivity and reduction of the PL decay time with increasing temperature are
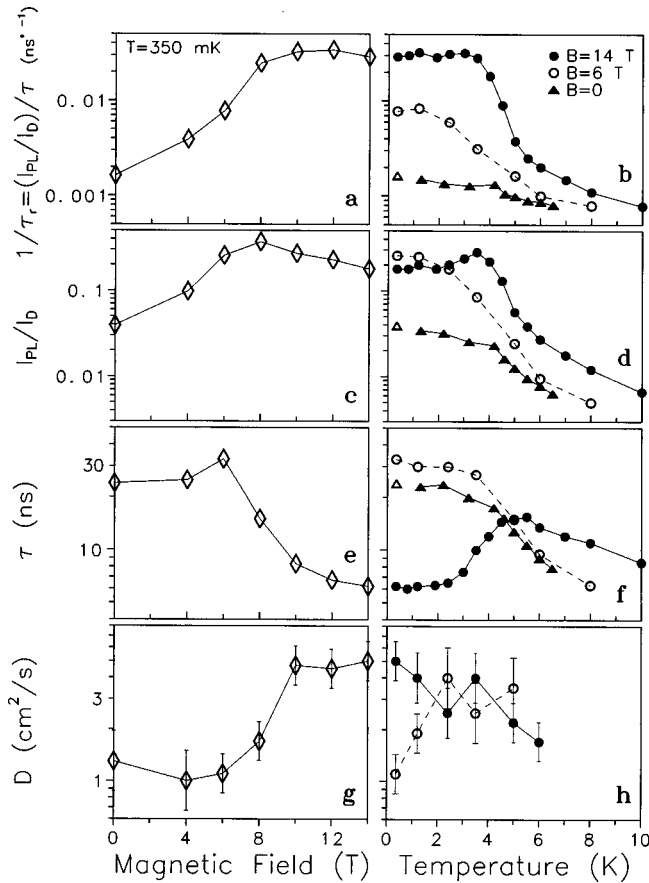
FIG. 9. Magnetic-field dependence of the radiative decay rate of indirect excitons in the AlAs/GaAs CQW (sample $S2$) in the indirect regime ($V_g=0$) $\tau_r^{-1}=(I_{PL}/I_D)\tau^{-1}$ (a), the integrated PL intensity of indirect excitons normalized to the integrated PL intensity in the direct regime I_{PL}/I_D (c), the initial decay time τ (e), and the exciton diffusion coefficient D measured by the time-of-flight technique (g) at $T=350$ mK and $W_{ex}=10$ W/cm^2. The temperature dependence of $\tau_r^{-1}=(I_{PL}/I_D)\tau^{-1}$ (b), I_{PL}/I_D (d), τ (f), and D (h) at $V_g=0$, $W_{ex}=10$ W/cm^2, and $B=0$, 6 and 14 T.

and superfluid lakes, with boundaries determined by the in-plane potential profile, is expected to be formed. A superfluid lake can include a number of weakly coupled condensate puddles; the total size of the lake is determined by the extension of a coherence between the puddles. This system is analogous to a random Josephson-junction array in superconductors. On a large scale, the exciton transport is the transport in a disordered array of normal and superfluid regions. The measured exciton transport parameters are averaged over the normal and superfluid regions in the excitation spot; the relatively low value of D characteristic of the observed rapid exciton transport can be understood in such a picture.

Note that the simulation of exciton transport by a diffusion equation with a single diffusion coefficient is certainly not valid for superfluid excitons. In the absence of a random potential, the spatial expansion of a 3D superfluid exciton cloud was described by the Gross-Pitaevskii equation in Ref. 68; a similar consideration for 2D excitons for the mask configuration considered in the paper will be reported elsewhere.[69] For the random array of normal and superfluid regions, the spatial extension of the exciton cloud is more complicated problem which was not considered theoretically. The value of D obtained above from the fitting of the exciton cloud extension process by the diffusion equation with a single diffusion coefficient presents a qualitative variation of the exciton transport, i.e., an increase or reduction of the exciton diffusivity with a variation of temperature and magnetic field.

Exciton superfluidity should disappear with a reduction of the exciton density at a critical density which is temperature, magnetic field, and disorder dependent. Due to the low level of the PL signal from the masked part of the sample, we have used only the maximum excitation power of the laser which corresponds to an average initial exciton density $\sim 10^{10}$ cm^{-2} (estimated from the excitation density and exciton lifetime); we were not able to measure the excitation density dependence by the time-of-flight technique. Indirectly, the exciton density dependence is revealed in the time evolution of the PL decay (the excitation density dependence of the PL decay is discussed below). At low temperatures and high magnetic fields, a rapid initial decay corresponding to the rapid exciton transport is observed until the exciton density drops down by several times; the subsequent decay is slow, and corresponds to slow exciton transport (Figs. 4, 6, and 8). The transition from the rapid initial to the slow subsequent exciton decay and transport is sharp, and corresponds to the expected disappearance of the exciton superfluidity.

At all studied magnetic fields, the temperature and magnetic-field dependences of the slow PL decay at large delay times are qualitatively similar to those of the initial PL decay at low magnetic fields: the differential decay time increases monotonically with increasing magnetic field, and reduces with increasing temperature (Figs. 4, 7, and 8). This implies similar exciton transport mechanisms in these two cases. The difference is in the stronger exciton localization for the former case: with increasing delay time more and more strongly localized excitons dominate the recombination, which results in a monotonic reduction of the decay rate. The increase of the exciton localization with delay time is mainly because excitons reach deep potential minima at their migration in the QW plane. Therefore, the exciton

due to the thermal exciton delocalization from the random potential minima, and the increase of the phonon-assisted tunneling probability, and has been observed at $B=0$ in AlAs/GaAs type-II superlattices and CQW's.[61,63,64] The monotonic reduction of the exciton diffusivity with increasing magnetic field can be qualitatively explained by the increase of the magnetoexciton mass, and is in qualitative agreement with the theoretical consideration of single exciton transport in AlAs/GaAs CQW's.[55] The reduction of the exciton diffusivity with increasing magnetic field has also been observed for direct excitons in GaAs/Al$_x$Ga$_{1-x}$As single QW's.[67]

The strong increase of D which is observed at high magnetic fields $B\gtrsim 6$ T and low temperatures $T\lesssim 4$ K [Figs. 9(e)–9(h)] can not be explained in terms of single exciton transport. A possible explanation for this effect, the validity of which is argued below, is the onset of exciton superfluidity. With increasing temperature the rapid exciton transport disappears, and at $T\gtrsim 5$ K the usual increase of the exciton diffusivity with temperature is recovered [Fig. 9(f)].

As discussed above, for exciton condensation in the presence of a random potential a random array of normal areas

transport results in an exciton energy relaxation and conse-
quent reduction of the spatially integrated exciton PL
energy.[70] We have found that the exciton energy relaxation
rate is increased with an increase of the exciton diffusivity
for all studied temperatures and magnetic fields, both for
normal and anomalously rapid exciton transport.[60] At the
same time the shift of the spatially integrated exciton PL
energy with delay time was found to be small enough to have
no influence on the measurements of τ and D with the PL
intensity integration within the 3-meV spectral range used in
the present paper.

At a large delay time due to the strong exciton localiza-
tion, τ_{nr} may exceed τ_r. Under this condition the total decay
rate will be mainly determined by the radiative recombina-
tion. This regime of strong exciton localization is not con-
sidered in this paper. Note that the monotonic increase of the
decay time with increasing magnetic field, and its reduction
with increasing temperature, is also characteristic of the ra-
diative decay of electrons and holes separately localized in
different in-plane potential minima; although their contribu-
tion to the integrated PL intensity is negligible, it is increased
with delay time, and may become essential at large delays.

Below, we briefly discuss possible contributions of other
mechanisms to the increase of the exciton diffusivity with
magnetic field, and its reduction with temperature. The
magnetic-field-induced suppression of the destructive inter-
ference between exciton paths could result in an increase of
the exciton diffusivity with magnetic field, in analogy to the
negative magnetoresistance in electron transport.[71,72] How-
ever, it seems unlikely that this mechanism contributes sig-
nificantly to the large increase of the exciton diffusivity ob-
served in our experiment due to the total charge neutrality of
excitons. Although theoretical consideration of the 2D exci-
ton transport in high magnetic fields in a strong random po-
tential (which corresponds to the exciton transport in CQW's
studied) is absent, the interference between exciton paths for
the 2D magnetoexciton transport in a weak disorder was con-
sidered in Ref. 73. A possibility of positive magnetodiffusion
was found at low magnetic fields ($l_B \gg a_B$), while at higher
fields the exciton diffusivity was found to reduce with a
magnetic field.[73] This is in a contradiction to the observed
reduction of the exciton diffusivity at low fields, and its in-
crease at high fields, and indicates, therefore, a small contri-
bution of the interference between exciton paths to the ob-
served variations of the exciton diffusivity.

The decrease of the exciton diffusivity with temperature is
characteristic of a phonon-wind-driven expansion of the ex-
citon cloud. This mechanism was suggested in Ref. 74 as an
explanation (alternative to the exciton superfluidity) for the
rapid exciton transport observed in experiments in Cu_2O.[10]
In our experiments the phonon wind cannot efficiently con-
tribute to the 2D exciton transport, because the fraction of
phonons propagating in the plane of the studied single nar-
row CQW is small. Furthermore, in measurements of the PL
decay in the unmasked part of the sample, the variations of τ
are not connected with the expansion of the exciton cloud as
they occur inside the excitation spot.

Besides the exciton superfluidity, another signature of the
exciton condensation is the onset of exciton superradiance
characterized by an increase of the exciton radiative decay
rate (see Sec. I). The indirect excitons in the CQW's studied

are of the X_z type, and are constructed from both electron
and hole bands with the minima at $k=0$; i.e., they are direct
in x-y momentum space. These excitons are also called
pseudodirect, their small exciton-photon coupling constant
and, correspondingly, small radiative decay rate, are due to
the fact that the electron state is constructed from the X_z
minima of 3D conduction band, and to the small overlap
between the electron and hole wave functions in the z direc-
tion. Therefore, arguments for the increase of the exciton
radiative decay rate at the exciton condensation (Sec. I) are
valid for indirect excitons in the considered AlAs/GaAs
CQW's.

The first data on the radiative decay rate of indirect exci-
tons in high magnetic fields were reported in Ref. 75. The
exciton radiative decay rate τ_r^{-1} can be directly derived from
the measured τ and the time-integrated exciton PL intensity
I_{PL}. In the case of monoexponential PL decay, τ_r^{-1}
$=(I_{PL}/G)\tau^{-1}$, where G is the generation rate. This formula
is already enough to show variations of τ_r^{-1}, but does not
present its absolute value, as G is unknown. For the estimate
of G the quantum efficiency of the PL in the direct regime
can be taken as unity. Then $G=I_D$ and $\tau_r^{-1}=(I_{PL}/I_D)\tau^{-1}$,
where I_D is the integrated PL intensity in the direct regime
measured at the same excitation. The magnetic field and tem-
perature dependences of τ_r^{-1} are shown in Figs. 9(a) and 9(b)
[$ns*$ in Figs. 9(a) and 9(b) differ from ns by a numerical
factor equal to the quantum efficiency in the direct regime,
which is unknown]. It was found that the nonexponentiality
of the PL decay introduces only unimportant quantitative
corrections to the dependences (see Appendix A). Note also
that the generation rate G is entirely determined by the ex-
citation density and is independent of temperature and mag-
netic field, this can be seen from the constant value of the
direct exciton PL intensity in the direct regime (Figs. 4, 7,
and 8).

At $T=350$ mK, τ_r^{-1} strongly increases with magnetic
field [Fig. 9(a)]. At high fields, τ_r^{-1} strongly drops down
with temperature around $T=4$ K, while at $B=0$ it only
weakly depends on temperature [Fig. 9(b)].

The observed dependences are discussed below. We be-
lieve that the radiative decay in our sample is entirely spon-
taneous, and that there is no contribution of the laser effects
to the observed variations of τ_r^{-1} (due to the small coupling
between the photon and indirect exciton, the antiwaveguide
character of the structure with a single CQW in the middle of
an 80-nm $Al_{0.48}Ga_{0.52}As$ layer surrounded by GaAs layers,
the small exciton density $\lesssim 10^{10}$ cm^{-2}, and the experiment
geometry, emitted light is collected in the direction perpen-
dicular to the CQW plane). The anomalously large τ_r^{-1} ob-
served at high magnetic fields and low temperatures is con-
sistent with the large radiative decay rate expected for the
exciton condensate discussed above. As in the case of the
exciton transport measurements, in our experiments the av-
erage value of τ_r^{-1} (integrated over the sample area) is mea-
sured. The increase of τ_r^{-1} in the condensate lakes is ex-
pected to be higher than the measured average value.

Note, however, that an increase of τ_r^{-1} with a reduction of
temperature and an increase of magnetic field is also ex-
pected for normal uncondensed excitons, but with a much
smaller magnitude compared to that observed at high mag-

netic fields and low temperatures. An increase of the uncondensed exciton oscillator strength (radiative decay rate) with magnetic field is due to the shrinkage of the relative in-plane e-h wave function.[21] According to calculations in Ref. 76, this should be only about two times for the increase of the magnetic field from 0 to 14 T for the considered CQW's. This value is close to the observed increase of τ_r^{-1} at high temperatures, >6 K, and is much smaller than that observed at low temperatures, <3 K [Fig. 9(b)]. An increase of the radiative decay rate of normal uncondensed excitons with a reduction of temperature is due to the gradual increase of the $k<k_0$ exciton state filling and the normal exciton coherent area;[47-52] it is presented by the increase of τ_r^{-1} at $B=0$, and is much smaller than the sharp increase of the radiative decay rate observed at high magnetic fields around $T=4$ K [Fig. 9(b)].

Note that the exciton transport and the exciton radiative decay rate are not decoupled for a system with a spatially inhomogeneous radiative decay rate. For the case of exciton condensation in a random potential, the spatial inhomogeneity of the radiative decay rate already follows from the existence of normal and condensed areas; see above. For the case of normal uncondensed excitons the radiative decay rate of indirect excitons is also inhomogeneous in the CQW plane. It depends on the strength of the Γ-X coupling, which is increased with a reduction of the energy splitting between direct and indirect excitons, and on the exciton coherent area, which is determined by the exciton localization length; see above. Therefore, the lateral fluctuations of the GaAs and AlAs layer thicknesses result in the inhomogeneity of the indirect exciton radiative decay rate in the CQW plane. In simplified terms the regions of higher radiative decay rate can be considered as radiative centers (RC's). The increase of the exciton diffusivity can result in more effective exciton transport to RC's and to a consequent increase of the radiative decay rate. We believe, however, that the contribution of the coupling between the exciton transport and radiative decay rate to the measured dependences of τ_r^{-1} [Figs. 9(a) and 9(b)] is small, and can be neglected for a qualitative understanding of the dependences. In some parameter range the relative variation of the exciton diffusivity and τ_r^{-1} is opposite to that expected from the coupling between them, which indicates the relatively small role of the coupling: first, with increasing magnetic field at $B \lesssim 6$ T the exciton diffusivity is reduced [Fig. 9(e)] but τ_r^{-1} is increased [Fig. 9(a)]; second, with increasing temperature at small fields the exciton diffusivity is increased [Fig. 9(f)], but τ_r^{-1} is reduced [Fig. 9(b)]. Note that the GaAs natural quantum dots for direct excitons[77] can also be considered as RC's, their relation to the indirect exciton transport is considered in Appendix B.

For an understanding of the observed anomalous rapid exciton transport and high exciton radiative decay rate, and their comparison with the expected properties of the exciton condensate, their variation in a complete parameter space should be measured and compared with the expected phase diagram of the exciton condensate. In a homogeneous 2D exciton system at high magnetic fields, the relation between the critical temperature, magnetic field, and density is given by the LL-KH formula for $T_{cB}(n,B)$; see Sec. I. A strong increase of τ_r^{-1} due to the exciton condensate superradiance

should appear at T_{cB}, as T_{cB} corresponds to the formation of the quasicondensate.[19] A local exciton superfluidity also appears at T_{cB}, while a macroscopic superfluid density appears at T_{KT}.[13] The temperature range $T_{KT}<T \lesssim T_{cB}$, characterized by the existence of unbound vortices resulting in a flow energy dissipation, increases with magnetic field: for a fixed exciton density, T_{cB} increases, while T_{KT} reduces with B;[19] see Sec. I. The local exciton superfluidity can be revealed in the measurements of the exciton diffusion on a small length scale which increases with a reduction of temperature.[78] In the present experiments the exciton transport on a microscopic scale (the diffusion length $\sqrt{D\tau} \sim 2$ μm) is considered. Therefore, we believe that the observed onset of the rapid exciton transport corresponds to T_{cB}, not T_{KT}.

The measured value of τ and the derived value of τ_r^{-1} are presented in Fig. 10 in a diagram form for a broad range of magnetic fields, temperatures, and excitation densities. The area of the circles in the left column of Fig. 10 is proportional to τ_r^{-1}, while the diameter of the circles in the right column of Fig. 10 is proportional to τ. As shown above, the measured τ is determined by the exciton diffusivity at all studied magnetic fields and temperatures. Based on the assumption that this relation also remains valid for all studied exciton densities, we believe that the right column of Fig. 10 presents the exciton transport variations with the larger circle corresponding to the smaller exciton diffusivity.

We first consider the data at the maximum excitation density studied, $W_{ex}=W_0=10$ W/cm^2, which corresponds to the upper planes of the diagram of Fig. 10. The upper left plane of Fig. 10 shows that τ_r^{-1} is increased with reducing temperature and increasing magnetic field, with a huge increase at low T and high B: the variation of τ_r^{-1} reaches about 60 times when going from the lower right corner to the upper left corner of the diagram plane. Because the strong increase of τ_r^{-1} is observed at the expected conditions for the exciton condensation, i.e., at low temperatures and high magnetic fields, and because this increase is expected for the exciton condensation and cannot be explained for normal uncondensed excitons, we believe that the observed huge increase of τ_r^{-1} corresponds to the exciton condensate superradiance. Conversely, the small increase of τ_r^{-1} observed with increasing magnetic field at high temperatures, $\gtrsim 5$ K, corresponds to the shrinkage of the in plane relative e-h wave function, while the small increase of τ_r^{-1} observed with reducing temperature at low magnetic fields, $B \lesssim 4$ T, corresponds to the gradual increase of $k<k_0$ state filling and the coherent area for normal uncondensed excitons; see above.

The upper right plane of Fig. 10 shows that, starting from high temperatures and low magnetic fields (lower right corner of the diagram plane), the exciton diffusivity is first reduced with increasing magnetic field and reducing temperature. This behavior corresponds to normal exciton transport in a random potential; see above. However, at the lowest temperatures and highest magnetic fields studied (upper left corner of the diagram plane), a strong increase of the exciton diffusivity is observed. Because this increase of the exciton diffusivity is observed at the expected conditions for the exciton condensation, i.e., at low temperatures and high magnetic fields, and because this increase is expected for the exciton condensation and cannot be explained for normal
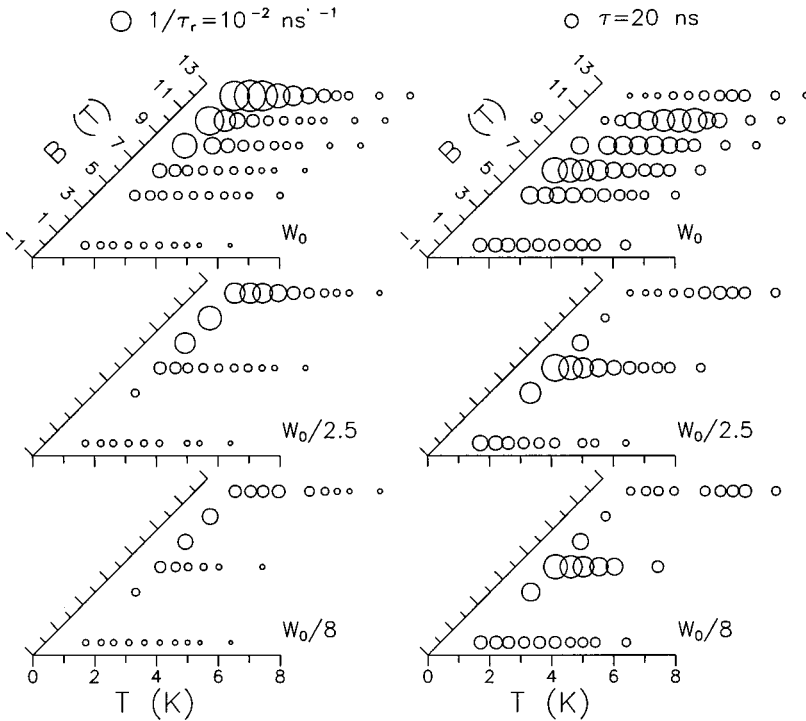
FIG. 10. Temperature, magnetic-field, and excitation density dependences of the radiative decay rate τ_r^{-1} (left column) and the initial decay time τ (right column) for indirect excitons in the AlAs/GaAs CQW (sample $S3$) in a diagram form: τ_r^{-1} is proportional to the area of the circles in the left column, τ is proportional to the diameter of the circles in the right column. The variations of τ reflect the changes of the exciton diffusivity, with the larger circle corresponding to the smaller exciton diffusivity; see text. $W_0 = 10$ W/cm^2.

uncondensed excitons, we believe that the observed strong increase of exciton diffusivity corresponds to the onset of superfluidity of the exciton condensate.

The anomalous rapid exciton transport and large τ_r^{-1} are observed in approximately the same range of parameters—at low temperatures and high magnetic fields, i.e., in the upper left corner of the diagram planes (Fig. 10). With an increase of temperature the critical magnetic field, at which the anomalous rapid exciton transport and large τ_r^{-1} are observed, is increased (from about 8 T at $T = 1.3$ K to about 12 T at $T = 4$ K); see Fig. 10. This variation qualitatively corresponds to that expected from the LL-KH formula. The absolute value of the critical temperatures are about an order of magnitude smaller than that expected from the LL-KH formula (Fig. 1). This discrepancy can be connected with the high-magnetic-field approximation used in the LL-KH theory, which results in the overestimation of the critical temperature. Note also that Fig. 1 presents the critical temperature for the condensation of single-layer two-dimensional excitons; taking into account the finite well thickness and spatial separation between the electron and the hole layers should result in a reduction of T_{cB}. As the disorder was not included in the LL-KH theory, this can also result in a discrepancy between the experiment and theory. Note that comparison with the LL-KH formula should be done carefully, as the exciton density itself depends on the temperature and magnetic field for the fixed W_{ex} (the exciton density is proportional to τ, which depends on temperature and magnetic field). The smoothness of the anomalous rapid exciton transport and large τ_r^{-1} onsets seems to be mainly determined by the random potential, which results in the critical parameter inhomogeneity in the CQW plane.

As pointed out above, with a reduction of the exciton density the exciton condensate and, correspondingly, the exciton superfluidity and superradiance, should disappear at some critical density. The density dependence of the exciton

diffusivity and τ_r^{-1} is presented by the lower two planes of the diagram which correspond to $W_{ex} = W_0/2.5$ and $W_0/8$. Figure 10 shows that the anomalously large exciton diffusivity and τ_r^{-1} observed at high magnetic fields and low temperatures (upper left corner of the diagram planes) are strongly reduced with the reduction of W_{ex} (while at low magnetic fields and high temperatures the exciton diffusivity and τ_r^{-1} only weakly depend on W_{ex}).

Although the reduction of the anomalously large exciton diffusivity and τ_r^{-1} with the reduction of W_{ex} qualitatively corresponds to the expected disappearance of the exciton superfluidity and superradiance, the observed excitation density dependence differs from that expected for the exciton condensation in a homogeneous 2D system. Even at lowest $W_{ex} = W_0/8$ an anomalously large exciton diffusivity and τ_r^{-1} (although being smaller than at high W_{ex}) are observed at approximately the same range of temperatures and magnetic fields as at $W_{ex} = W_0$, see Fig. 10. This contradicts the LL-KH formula, which implies a reduction of the critical temperature and an increase of the critical magnetic field with a reduction of exciton density. We do not have a clear understanding of the observed independence of the critical temperature and magnetic field from exciton density. However, we suppose that it might be specific for the exciton condensate in a random potential, and we discuss this assumption below. In the presence of a random potential, excitons are collected in local potential minima, forming lakes with an exciton density larger than the average density. The later was estimated to be about 10^{10} cm^{-2} for $W_{ex} = W_0$. With a reduction of temperature the exciton condensation first occurs at lakes with a higher exciton density and smaller local potential fluctuations. We suppose that an increase of the average exciton density with W_{ex} results only in a weak increase of the exciton density in the lake because of an increase of the exciton density outside the lake, and because
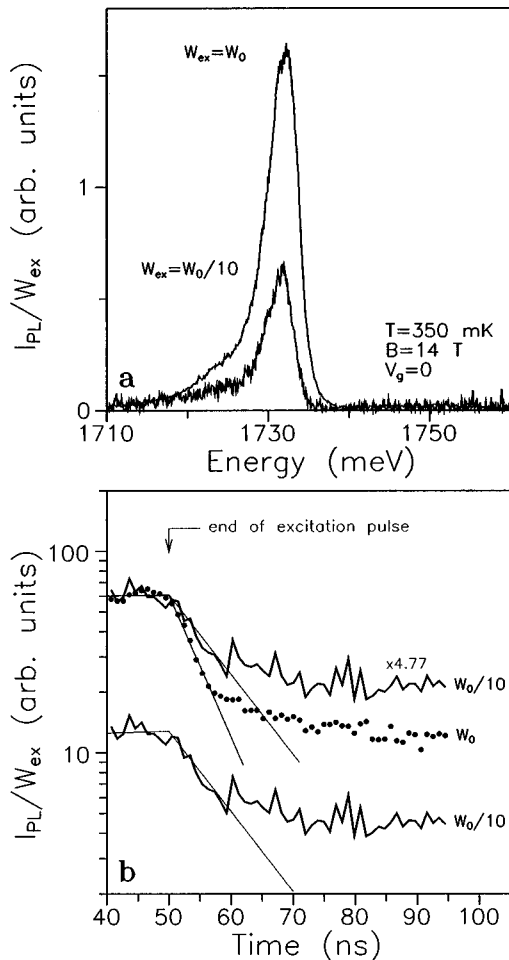
FIG. 11. The time-integrated PL spectra (a) and the decay curves (b) of indirect excitons in the AlAs/GaAs CQW (sample $S2$) at $T=350$ mK, $V_g=0$, and $B=14$ T for excitation densities $W_{ex} = W_0 = 10$ W/cm^2 and $W_{ex} = W_0/10$. The PL intensities are normalized to W_{ex}. The normalized decay curve at $W_{ex} = W_0/10$, multiplied by 4.77, is also shown for comparison with the decay at $W = W_0$.

of an increase of the lake lateral size due to the screening of the random potential. This proposed weak dependence of the exciton density in the lakes on W_{ex} may explain the observed independence of the critical temperature and magnetic field on W_{ex}.

The variation of the PL decay and spectrum at high magnetic fields and low temperatures with excitation density is shown in Fig. 11. Note that, at high magnetic fields and low temperatures, the increase of the radiative decay rate with increasing exciton density is larger than the increase of the nonradiative decay rate; this results in a superlinear increase of the exciton PL intensity with the excitation density (Fig. 11).

In this paragraph we discuss the relation between the decrease of the anomalously large exciton diffusivity with delay time and with W_{ex} reduction. With increasing delay time at $W_{ex} = W_0$, the rapid exciton decay/transport disappears when the exciton PL intensity drops by about four times, which corresponds to the reduction of the exciton density by not more than four times (Fig. 11). With a reduction of W_{ex} by ten times, which corresponds to the reduction of the ex-

citon density by about five times (taking into account two times increase of τ), the rapid exciton decay/transport is still observed, but becomes slower and disappears when the exciton PL intensity drops only about two times (Fig. 11). Therefore, the difference between the effect of exciton density reduction with decreasing W_{ex}, and with delay time on the exciton decay and transport, is not large. We suppose that the difference can be connected to the following: with delay time excitons reach deep local potential minima and localize there, this increase of the exciton localization also results in the slowing of the rapid exciton decay and transport with delay time.

The variations of τ, the exciton diffusivity obtained by the time-of-flight technique, and τ_r^{-1}, are qualitatively similar for different Γ-X_z AlAs/GaAs CQW's studied if the CQW samples are characterized by relatively small potential fluctuations which are revealed in the small PL linewidth. As pointed out in Sec. I, an increase of potential fluctuations should result in a reduction of the condensate lakes' lateral sizes and, ultimately, in the destruction of the exciton condensate. The variation of the measured parameters, in particular a disappearance of the rapid exciton decay and transport under the sample degradation which results in an increase of potential fluctuations, is considered in Appendix C.

IV. VARIATION OF EXCITON PL DECAY WITH GATE VOLTAGE. STRONGLY INDIRECT REGIME

In Sec. III, indirect excitons at $V_g=0$ were considered. The gated CQW's studied allow one to follow the variation of the measured quantities with the gate voltage. In particular, a more indirect regime is realized at negative V_g, which is characterized by a lower transition energy (Fig. 3) and a longer decay time for indirect excitons. This more indirect regime is considered in this section.

The magnetic-field dependence of the indirect exciton PL decay and spectrum at $V_g=-0.8$ V and $T=350$ mK is shown in Fig. 12. The temperature dependence of the indirect exciton PL decay at $V_g=-0.8$ V for $B=6$ and 14 T is shown in Fig. 13. The corresponding temperature and magnetic-field dependences of the indirect exciton initial decay time, integrated indirect exciton PL intensity normalized to the PL intensity in the direct regime, and derived radiative decay rate are shown in Fig. 14. Qualitatively the dependences are similar to those observed at $V_g=0$. The low level of the PL intensity from the masked part of the sample at negative V_g did not allow us to measure the exciton diffusivity directly by the time-of-flight technique. Similar to the $V_g=0$ case, in the strongly indirect regime the measured decay time is approximately equal to τ_{nr}. We believe that the relation between τ and the exciton diffusivity also remains valid in the strongly indirect regime, in analogy with $V_g=0$ data. The drop of τ with increasing magnetic field at $T=350$ mK is more pronounced in the strongly indirect regime compared to the $V_g=0$ case: at $V_g=-0.8$ V the initial decay time is reduced 14 times between 10 and 14 T [Fig. 14(e)], by comparison, at $V_g=0$ the reduction of τ between 6 and 14 T is only five times [Fig. 9(e)]. Also the drop of τ with decreasing temperature at $B=14$ T is more pronounced in the strongly indirect regime: between 5 and 3 K the initial
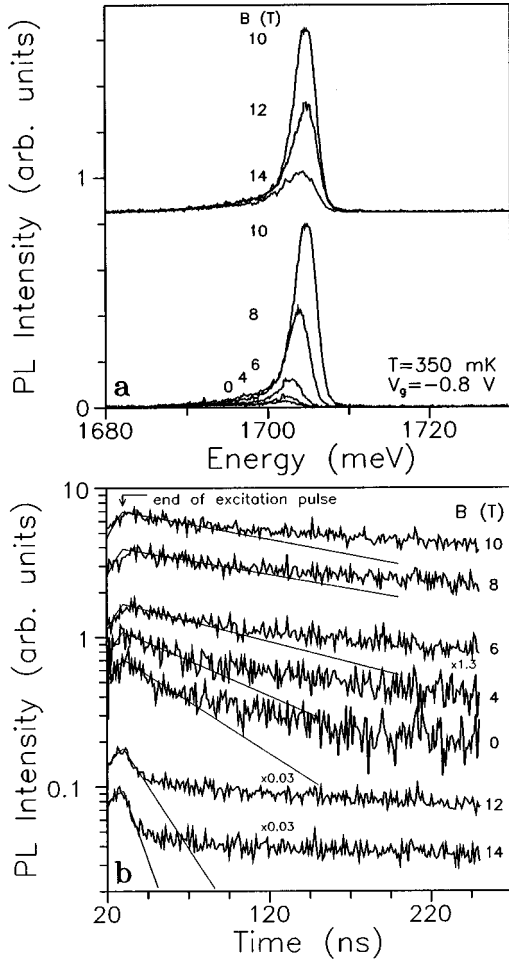
FIG. 12. Magnetic-field dependence of the time-integrated PL spectrum (a) and the PL decay (b) of indirect excitons in the AlAs/GaAs CQW (sample $S2$) in the strongly indirect regime ($V_g = -0.8$ V) at $T = 350$ mK and $W_{ex} = 10$ W/cm^2 (pulse duration 30 ns). Thin lines are the fitting curves for the initial times of the PL decay.
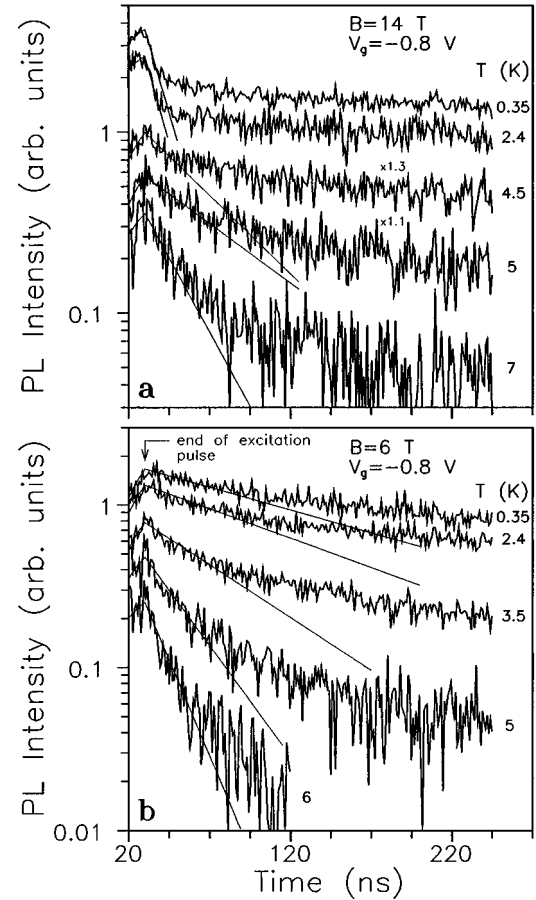

FIG. 13. Temperature dependence of the PL decay of indirect excitons in the AlAs/GaAs CQW (sample $S2$) in the strongly indirect regime ($V_g = -0.8$ V) at $W_{ex} = 10$ W/cm^2 (pulse duration 30 ns), $B = 14$ T (a) and 6 T (b). Thin lines are the fitting curves for initial times of the PL decay.

decay time is reduced four times for $V_g = -0.8$ V [Fig. 14(f)], and only by two times for $V_g = 0$ [Fig. 9(f)]. This indicates a strong increase of the exciton diffusivity at low temperatures and high magnetic fields at $V_g = -0.8$ V.

Qualitatively similar magnetic-field dependences of the indirect exciton PL decay were observed at all gate voltages studied. The magnetic-field dependences of the indirect exciton initial PL decay time and integrated indirect exciton PL intensity normalized to the PL intensity in the direct regime are shown in Fig. 15 for different V_g's. At all studied V_g's, the initial PL decay time and integrated PL intensity of indirect excitons first increase and then reduce with increasing magnetic field. The variations are similar to those at $V_g = 0$, and are connected with the magnetic-field dependence of radiative and nonradiative decay rates. Note that the magnetic field corresponding to the beginning of the drop of τ, i.e., to the onset of the anomalously rapid indirect exciton transport, depends nonmonotonically on V_g [Fig. 15(c)]. The critical magnetic field corresponding to the onset of the rapid exciton transport is close to the field at which the maximum of the indirect exciton PL intensity is observed, B_{max} [compare Figs. 15(b) and 15(c)]. The gate voltage dependence of B_{max} is shown in Fig. 15(a). Note that Fig. 15(a) presents the data

obtained at cw excitation. Although the gate voltage dependence of B_{max} is qualitatively similar for cw and pulsed excitations, B_{max} is slightly higher at cw excitation for all V_g's [compare Figs. 15(a) and 15(b)]. Presumably this is due to a larger heating of the exciton system at cw excitation, resulting in an increase of the critical magnetic field (as an increase of temperature results in the increase of the critical magnetic field, see Fig. 10). The shape of the observed gate voltage dependence of the critical magnetic field, characterized by the minimum at $V_g = 0$, is not clear. We assume that the reduction of the critical magnetic field at $-1.2 V < V_g < -0.5$ V and $0 < V_g < 0.2$ V (no pronounced maxima in the integrated PL intensity was observed at $V_g > 0.2$ V, due to approaching the direct regime) can be connected with the gradual transition to a more and more indirect regime, which improves critical conditions for the exciton condensation. We also assume that the local minimum of the critical magnetic field at $V_g = 0$ can be connected with the local minimum of the potential fluctuations, e.g., due to the absence of an electric-field inhomogeneity in the z direction caused by the gate operation unperfectness, as well as with a reduction of an electric current across the CQW structure in the z direction. The effect of a random potential was discussed above. The large current through the condensate lake may destroy the condensate due to the heating effects,
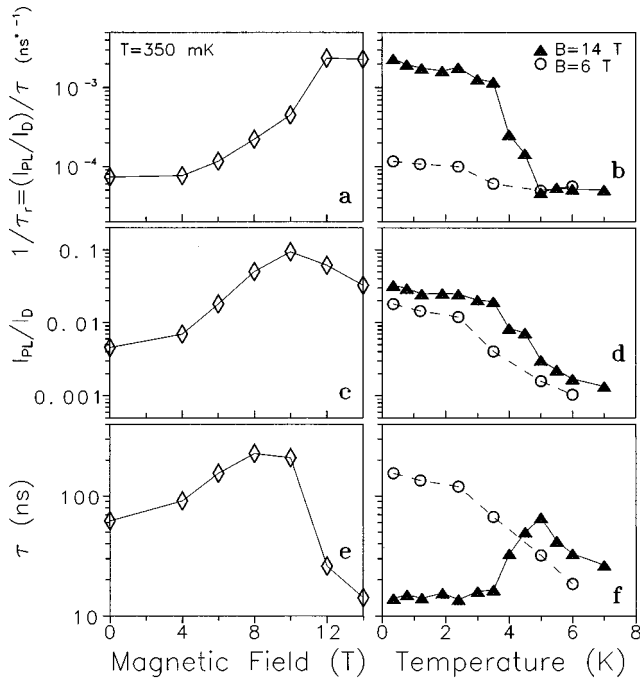
FIG. 14. Magnetic-field dependence of the radiative decay rate of indirect excitons in the AlAs/GaAs CQW (sample $S2$) in the strongly indirect regime ($V_g = -0.8$ V) $\tau_r^{-1} = (I_{PL}/I_D)\tau^{-1}$ (a), the integrated PL intensity of indirect excitons normalized to the integrated PL intensity in the direct regime I_{PL}/I_D (c), and the initial decay time τ (e) at $T = 350$ mK and $W_{ex} = 10$ W/cm^2. The temperature dependence of $\tau_r^{-1} = (I_{PL}/I_D)\tau^{-1}$ (b), I_{PL}/I_D (d), and τ (f) at $V_g = -0.8$ V, $W_{ex} = 10$ W/cm^2, and $B = 6$ and 14 T.

and due to the increased deviation from a charge neutrality. Therefore, the reduction of both of the potential fluctuations and the electric current at $V_g = 0$ should improve the critical conditions for the exciton condensation. Note that the nonmonotonic gate voltage dependence of the critical magnetic field results in a nonmonotonic gate voltage dependence of the indirect exciton PL intensity and decay time at the fixed magnetic field (with the different shape at different B); see Fig. 15.

V. FLUCTUATIONS OF INDIRECT EXCITON PL INTENSITY

A spectacular effect has been observed under cw photoexcitation in high magnetic fields, namely, a huge broadband noise in the integrated PL intensity of indirect excitons.[59] Figure 16 shows the variation of the integrated PL intensity of indirect excitons with sweeping magnetic fields at $T = 350$ mk and $V_g = -0.5$ V. The average variation of the integrated PL intensity under cw photoexcitation is similar to that under pulsed photoexcitation: first an increase and then a reduction of I_{PL} is observed with increasing magnetic field. This is connected with variations of radiative and nonradiative decay times of indirect excitons (note that, for the determination of B_{max} in Sec. IV, the fluctuations in time were averaged). The power spectrum of the anomalously large noise has a broadband spectrum (right inset to Fig. 16). The noise is observed at low temperatures (left inset to Fig. 16). The spectral position of the PL line is practically constant during the intensity fluctuations (Fig. 17), which shows that
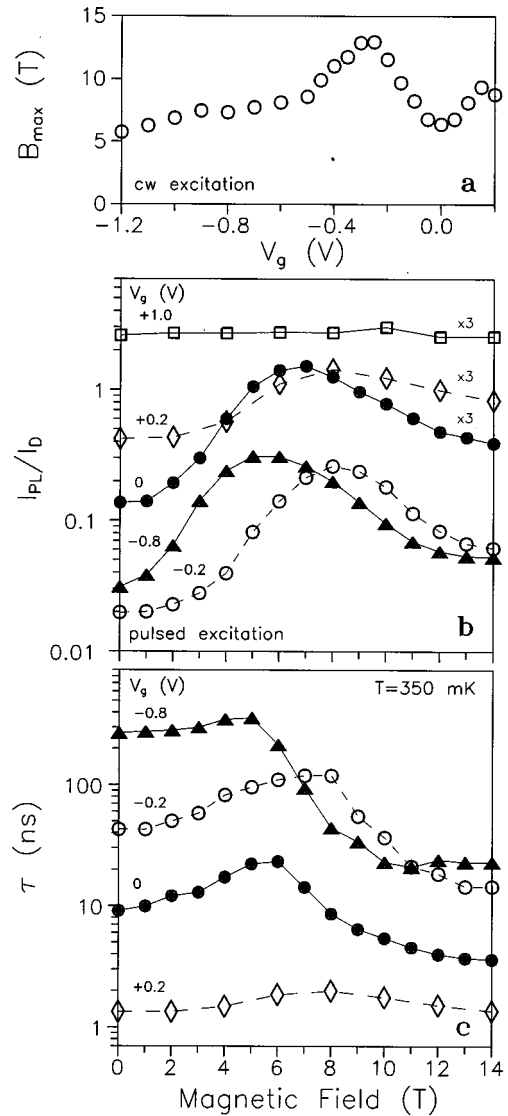

FIG. 15. Gate voltage dependence of the magnetic field corresponding to the maximum of the indirect exciton PL intensity in the AlAs/GaAs CQW (sample $S1$) at cw excitation at $T = 350$ mK (a). Magnetic-field dependence of the integrated PL intensity (b) and the initial decay time (c) of excitons in the AlAs/GaAs CQW (sample $S1$) at $T = 350$ mK for different gate voltages; the data at $V_g = +1$ V correspond to the direct exciton PL in the direct regime, while the data at all other V_g's correspond to the indirect exciton PL in the indirect regime.

the noise cannot be related to the fluctuations of the CQW potential profile in the z direction. The noise is observed only in the indirect regime. The amplitude of the noise is reproducible for the fixed parameter set.

The appearance of huge noise is strong evidence of the presence of coherence in the exciton system. The noise amplitude is known to be inversely proportional to the number of statistically independent entities in a system.[79] Large noise amplitudes therefore denote that only a small number of entities exists in the macroscopically large photoexcited region.

The appearance of these macroscopic entities in the exciton system is consistent with the exciton condensation. A condensed lake can be considered as one macroscopic entity. Due to the high radiative decay rate of the exciton condensate, the PL signal of condensed excitons is much higher as
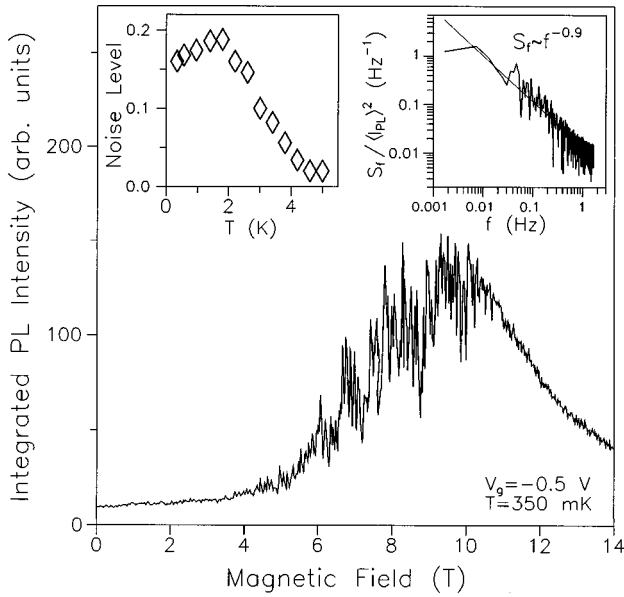
FIG. 16. Magnetic-field dependence of the integrated PL intensity of indirect excitons in the AlAs/GaAs CQW (sample $S1$) at cw excitation at $T = 350$ mK, $V_g = -0.5$ V, and $W_{ex} = 1$ W/cm^2. Left inset: temperature dependence of the noise level $\langle \delta I_{PL} \rangle / \langle I_{PL} \rangle$ at $B = 9$ T. Right inset: power spectrum of the noise.

compared to uncondensed ones. The formations and disappearances of condensate lakes therefore result in fluctuations of the total PL signal. Note that large fluctuations of the total PL signal are possible because of the small PL quantum efficiency of normal uncondensed indirect excitons, which can be strongly increased in the condensate lake sites at the exciton condensation. For the existence of broadband noise, the condensate lifetime in the lake site should have a broad distribution.[80] Note that the large noise amplitude is observed on a time scale longer than seconds (right inset to Fig.
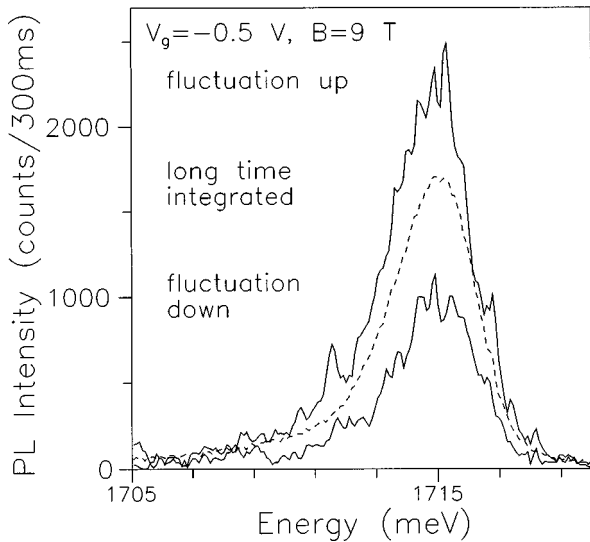

FIG. 17. Long-time-integrated indirect exciton PL spectrum and indirect exciton PL spectra integrated during 0.3 s in the noise regime at cw excitation at $B = 9$ T, $T = 350$ mK, $V_g = -0.5$ V, and $W_{ex} = 0.5$ W/cm^2 in the AlAs/GaAs CQW (sample $S1$). The spectra were measured by a CCD camera.

16). Therefore, under continuous photoexcitation the lifetime of the condensate lake is much longer than the exciton recombination time, which denotes that during its lifetime the condensate lake is in a quasiequilibrium: the exciton recombination is compensated by the exciton collection into the condensate. The mechanism of the appearance and disappearance of the condensate in the lake site is unknown. There is an indication that this is connected with the electric current across the CQW structure (which may destroy the condensate; see Sec. IV): the noise amplitude has a local minimum at $V_g = 0$. We tentatively suppose that variations of the current filament paths with time result in a fluctuation of the electric current across the condensate lake site, which causes the appearance or disappearance of the condensate in the site depending on the electric current magnitude.

The noise is observed only on the left slope of the $I_{PL}(B)$ dependence (Fig. 16), i.e., the noise appears in the range of magnetic fields where τ_r^{-1} starts to increase, and disappears in the range of magnetic fields where τ_r^{-1} saturates and rapid exciton transport is observed. Therefore, the noise can be understood as fluctuations near the phase transition connected with an unstability of the condensate lakes.

VI. CONCLUSIONS

The problem of exciton condensation (analogous to the Bose-Einstein condensation of bosons) in quantum-well structures was considered in this paper. The expected properties of the exciton condensate in QW's which can be detected in PL experiments were discussed. In particular, the condensation of two-dimensional excitons direct in x-y momentum space was argued to be accompanied by an increase of the exciton radiative decay rate. The qualitative influence of a random potential, which is unavoidable in QW's, on the exciton condensate properties was briefly discussed. The indirect excitons in AlAs/GaAs CQW's at high magnetic field were shown to be a good candidate for experimental observation of exciton condensation due to the combination of the long exciton lifetime, small spatial separation between the electron and hole layers, relatively small potential fluctuations in AlAs/GaAs CQW's, and the improvement of critical conditions for exciton condensation by a high magnetic field.

The transport and luminescence of longlife indirect excitons in AlAs/GaAs CQW's at conditions where the exciton condensation was theoretically predicted to occur, i.e., at low temperatures and high magnetic fields, were studied. A set of anomalies in the transport and luminescence of indirect excitons were observed at low temperatures and high magnetic fields: a large increase of the exciton diffusivity, a large increase of the exciton radiative decay rate, and a huge noise in the integrated exciton PL intensity. The observed anomalies were shown to be evidence of exciton condensation at low temperatures and high magnetic fields; that is they indicate the onset of superfluidity and superradiance of the exciton condensate. No explanation alternative to the exciton condensation was found for the observed anomalies. No anomalies were observed at zero magnetic field, which means that the critical conditions for the exciton condensation are not overcome for indirect excitons in the considered AlAs/GaAs CQW's at $B = 0$. As predicted theoretically, the role of the magnetic field is in the improvement of the critical condi-
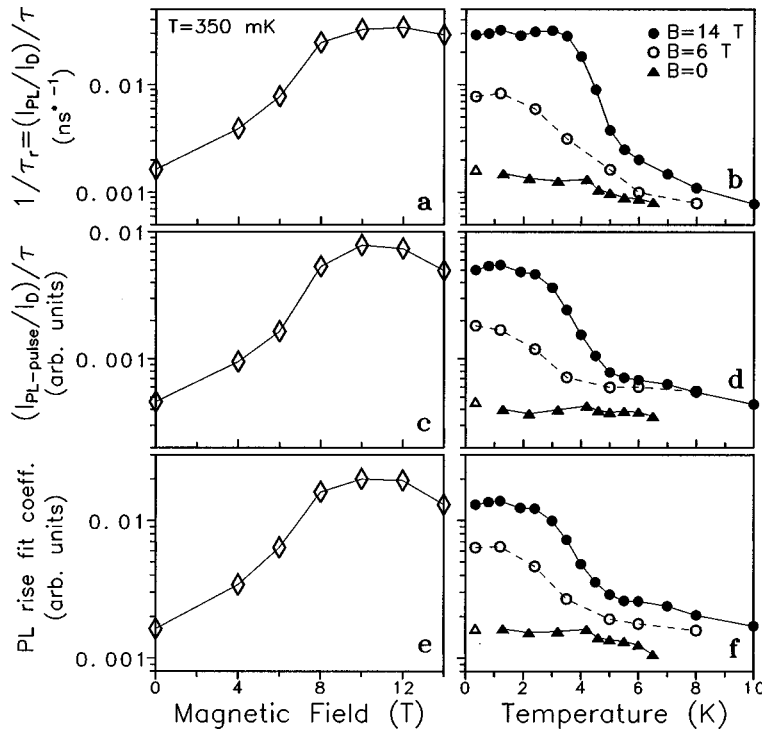
FIG. 18. Magnetic-field and temperature dependences of $\tau_r^{-1} = (I_{PL}/I_D)\tau^{-1}$ [(a) and (b)], $(I_{PL\text{-}pulse}/I_D)\tau^{-1}$, where $I_{PL\text{-}pulse}$ is the PL intensity integrated during the excitation pulse [(c) and (d)], and the PL rise fit coefficient, which is proportional to τ_r^{-1} for the PL rise characterized by one exponent (see text) [(e) and (f)], for indirect excitons in the AlAs/GaAs CQW (sample S2) at $V_g = 0$.

tions for the exciton condensation. The range of magnetic fields studied can be divided into three parts. At low magnetic fields both the exciton transport and the radiative decay rate are characteristic of normal uncondensed excitons in a random potential: the exciton diffusion coefficient is increased with increasing temperature, and the radiative decay rate only weakly depends on temperature. At the highest magnetic fields studied, both the exciton diffusion coefficient and the radiative decay rate are anomalously large, and drop with increasing temperature; this behavior is consistent with the expected exciton superfluidity and superradiance of the exciton condensate at low temperatures and high magnetic fields. At intermediate magnetic fields, a huge noise in the integrated PL intensity is observed under cw photoexcitation; the noise is consistent with fluctuations near the phase transition connected with an instability of the condensate lakes. The range of parameters (magnetic fields, temperatures, and exciton densities) for the existence of an exciton state characterized by an anomalously large exciton diffusivity and radiative decay rate was experimentally determined. It was found to be qualitatively consistent with the expected phase diagram of the exciton condensate in a random potential. For a complete understanding of the observed anomalies, the experimental data should be compared with a theory of the 2D exciton condensation in a random potential in finite magnetic fields, which is not developed at present.

APPENDIX A: NONEXPONENTIALITY OF PL DECAY AND EXCITON RADIATIVE DECAY RATE DERIVATION

In the case of monoexponential PL decay

$$\tau_r^{-1} = Q_D(I_{PL}/I_D)\tau^{-1}, \qquad (A1)$$

where the quantum efficiency in the direct regime, $Q_D = I_D/G$, can be taken as unity when the variation of τ_r^{-1}, but not its absolute value, is studied; see Sec. III. In this appendix we consider the influence of the nonexponentiality of the indirect exciton PL decay on the exciton radiative decay rate derivation.

The PL decay at large delay times is characterized by long differential decay times which differ from the initial decay time used for the derivation of τ_r^{-1} in Eq. (A1). This difference is especially large at low temperatures and high magnetic fields. In Eq. (A1), the integrated PL intensity, which includes the PL decay at a large delay time, is used. To understand the correction which is introduced by including the PL decay at large delay times in the above derivation of τ_r^{-1} we have completely excluded the PL decay after the excitation switching off from Eq. (A1). This was done (i) by replacing I_{PL} by $I_{PL\text{-}pulse}$ in Eq. (A1), which is the indirect exciton PL intensity integrated only during the 50-ns excitation pulse, and (ii) by fitting of the indirect exciton PL rise by the single-exponent rate equation with τ_r^{-1} as a fitting parameter (the deviations from the single-exponent PL rise at the initial times of the excitation pulse were disregarded, and

the fitting was done for the latest times of the excitation pulse; see the thin lines in Figs. 4, 7, and 8). Note that both these methods are not correct for the derivation of τ_r^{-1}, but they allow one to show that the nonexponentiality of the indirect exciton PL decay introduces only unimportant corrections to the variations of τ_r^{-1} derived by Eq. (A1).

The magnetic-field and temperature dependences of τ_r^{-1} $=(I_{PL}/I_D)\tau^{-1}$, $(I_{PL-pulse}/I_D)\tau^{-1}$, and the PL rise fit coefficient, which is proportional to τ_r^{-1} for a PL rise characterized by one exponent, are shown in Fig. 18. The dependences are qualitatively similar, and differ from each other only quantitatively. Therefore, the indirect exciton PL with a long delay time and, consequently, the nonexponentiality of the PL decay, results only in unimportant quantitative corrections to the variations of τ_r^{-1} derived by Eq. (A1). This is mainly due to the large magnitude of the radiative decay rate variations with magnetic field and temperature.

APPENDIX B: INDIRECT EXCITON TRANSPORT AND NATURAL QUANTUM DOTS

Zero-dimensional (0D) direct excitons in the GaAs QW localized in local deep potential minima caused by the interface fluctuations, i.e., in natural quantum dots (NQD's), may be in energy resonance with indirect excitons.[77] The emission spectrum of 0D direct excitons in NQD's has the shape of narrow lines characteristic of a 0D density of states. These lines can be separately resolved in the PL spectra with high spatial resolution, due to a small number of NQD's in the excitation spot. This number is effectively reduced in the indirect regime due to the resonant injection of carriers into the NQD's which are in energy resonance with indirect excitons.[77] The relation between the NQD emission and the observed anomalies in transport and luminescence of indirect excitons is discussed in this appendix.

The NQD's can be considered as radiative centers, discussed in Sec. III. Therefore, their PL intensity should be connected with the exciton diffusivity; see Sec. III. The magnetic-field dependence of the PL spectrum in the indirect regime ($V_g = -0.1$ V) at cw excitation with a small excitation spot (~ 100 μm^2) is shown in Fig. 19. The narrow lines which are seen on the background of the broad line correspond to the PL of direct excitons in NQD's, while the broad line corresponds to the indirect exciton PL. The condition at which the NQD emission can be resolved in the spectra, i.e., the small excitation spot and consequent high excitation density, is not optimal for the observation of the anomalously large exciton diffusivity and radiative decay rate, mainly due to a heating of the excitation spot and the too-high exciton density (for cw excitation with the large $\sim 150\times 150$-μm^2 excitation spot, the disappearance of the anomalies was observed at a high excitation level corresponding to the plasma regime). Still a small increase followed by a reduction of the indirect exciton PL intensity with magnetic field can be seen in Fig. 19. These variations of the indirect exciton PL intensity reflect the variations of the exciton transport and radiative decay rate, with the intensity maximum approximately corresponding to the onset of the rapid exciton transport; see Secs. III and IV. Figure 19 shows that at $B \lesssim B_{max} \approx 9$ T the intensity of NQD emission is decreased with increasing mag-
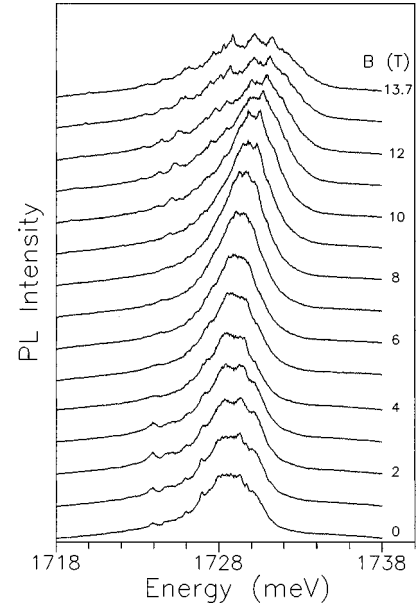

FIG. 19. Magnetic-field dependence of the PL spectra in the indirect regime ($V_g = -0.1$ V) at cw excitation with a small excitation spot (~ 100 μm^2) for the AlAs/GaAs CQW (sample $S1$). The narrow lines which are seen on the background of the broad line correspond to the PL of direct excitons in the natural quantum dots, while the broad line corresponds to the indirect exciton PL.

netic field, while at $B \gtrsim B_{max}$ it is increased with field. As shown in Sec. III, the exciton diffusivity is reduced at $B \lesssim B_{max}$, and increased at $B \gtrsim B_{max}$ with increasing B. Therefore, the increase (reduction) of the NQD PL intensity corresponds to the increase (reduction) of the exciton diffusivity. This corresponds to the expected behavior: the increase of the exciton diffusivity results in the more effective exciton transport to NQD's, and to the consequent increase of the NQD PL intensity.

Note that the contribution of the NQD emission to the magnetic field and temperature dependences of the indirect exciton radiative decay rate, discussed in Sec. III, is not crucial, and can be neglected for the qualitative understanding of the dependences. This is (i) due to the small influence of the coupling between the radiative centers and the exciton transport on the observed variations of the indirect exciton radiative decay rate which was discussed in Sec. III, and (ii) because the qualitatively similar dependences for the indirect exciton radiative decay rate are observed for all gate voltages studied (Secs. III and IV) which are characterized by the different energy separation between direct and indirect excitons and, consequently, very different amount of NQDs resonant to the indirect exciton energy (the NQD density is given by the density of localized states in the GaAs QW, which is quickly reduced with the energy reduction below the direct band edge[77]).

APPENDIX C: SAMPLE DEGRADATION

The studied AlAs/GaAs CQW samples were found to degrade with time. The degradation is strongly increased after a mesa is fabricated by lithography processing, and has a char-
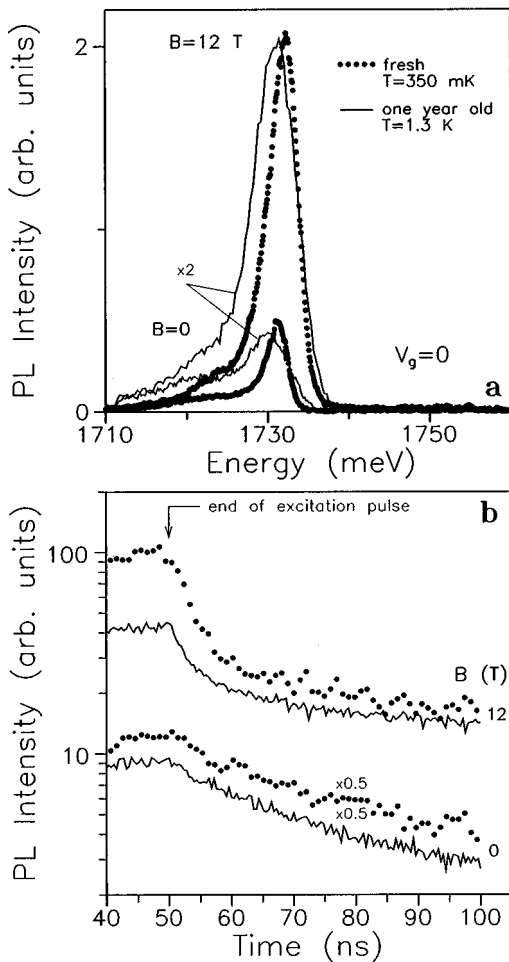
FIG. 20. Time-integrated PL spectra (a) and PL decay curves (b) of indirect excitons in the AlAs/GaAs CQW ($V_g=0$) for sample $S2$ measured just after the mesa processing (fresh); and sample $S3$, which is the same mesa measured about one year after the mesa processing (one year old). $W_{ex}=10$ W/cm^2, and the pulse duration is 50 ns.

acteristic degradation time of a year. The origin of the degradation is not clear. It is likely connected with the AlAs layer, as no analogous degradation was observed in CQW's of a type which do not contain the AlAs layer. The degradation manifests itself in an increase of the PL linewidth of indirect excitons; e.g., in one year the linewidth approximately doubles; see Fig. 20(a). This implies that the degradation results in an increase of the potential fluctuations in AlAs/GaAs CQW's.

The degradation limits the time for the experiments on the particular mesa; however, it also has some positive effect—it allows one to follow the variation of the measured quantities with an increase of the potential fluctuations (which is, however, uncontrollable). Figure 20(b) presents a comparison of the indirect exciton PL decay for sample $S2$, which was measured just after the mesa processing, and sample $S3$,

which is the same mesa as sample $S2$ but measured about one year after the mesa processing. The intensity is normalized to the direct exciton PL intensity, whose spectrum remains unchanged over a few years of observation. Figure 20(b) shows that the rapid exciton decay, corresponding to the anomalously rapid exciton transport, observed at high magnetic field ($B=12$ T in the figure) is strongly suppressed for sample $S3$ which is characterized by the large potential fluctuations. That is, with a delay time the rapid exciton decay and transport is more quickly changed by the slow exciton decay and transport for sample $S3$ compared to sample $S2$ [Fig. 20(b)]. The slow exciton decay implies the absence of the percolation between the superfluid lakes on a scale of the distance between NC's (or the absence of superfluid lakes at all). Therefore, the observed difference between samples $S2$ and $S3$ is consistent with the expected behavior of the exciton condensate in a random potential: for the larger potential fluctuations the percolation between the superfluid lakes (or the superfluid lakes themselves) disappears more quickly with the exciton decay, as the exciton condensate in the larger random potential is characterized by the smaller superfluid lakes; see Sec. I. The influence of the sample degradation on the PL decay in the normal regime ($B=0$) is relatively weak [Fig. 20(b)].

Note that the detailed diagram of Fig. 10 was measured for sample $S3$. The diagram for sample $S2$ is expected to have a sharper boundary between the state characterized by the anomalously large exciton diffusivity and the radiative decay rate, i.e., the exciton condensate, and the normal exciton state due to the smaller potential fluctuations (indications of this can be seen from a comparison of Figs. 9 and 10).

The noise in the integrated PL intensity of indirect excitons disappears first with the sample degradation. No noise was observed in sample $S3$, characterized by large potential fluctuations. The noise in sample $S1$ (which is a mesa processed a year before sample $S2$ from the same substrate, and measured just after the processing, indirect excitons in samples $S1$ and $S2$ have the same linewidth at the same external parameters and are characterized by the similar behavior) disappeared in about five months after the mesa processing; the new mesa processed after the noise disappearance in sample $S1$ from the same substrate and measured just after the processing still showed the noise, which was, however, reduced in amplitude, and was observed in the narrower parameter range. We have not performed cw experiments on sample $S2$. The disappearance of the noise prior to the disappearance of the anomalously large exciton diffusivity and radiative decay rate with increasing potential fluctuations is consistent with the expected behavior of the exciton condensate in a random potential: a large noise can be observed for a small number of large condensate lakes; the increase of potential fluctuations results in a reduction of the lake lateral sizes and, presumably, in an increase of their number, due to the dividing of the large lakes into several small lakes; this large number of smaller lakes can still result in an anomalously large exciton diffusivity and radiative decay rate.

[1] L. V. Keldysh and A. N. Kozlov, Zh. Éksp. Teor. Fiz. **54**, 978 (1968) [Sov. Phys. JETP **27**, 521 (1968)].

[2] L. V. Keldysh and Yu. E. Kopaev, Zh. Éksp. Teor. Fiz. **6**, 2791 (1964) [Sov. Phys. Solid State **6**, 6219 (1965)].

[3] C. Comte and P. Nozieres, J. Phys. **43**, 1069 (1982); P. Nozieres and C. Comte, *ibid.* **43**, 1083 (1982).

[4] M. Anderson, J. R. Fisher, M. R. Matthews, C. E. Wieman, and E. A. Cornell, Science **269**, 198 (1995).

[5] T. M. Rice, Solid State Phys. **32**, 1 (1977).

[6] D. Hulin, A. Mysyrowicz, and C. Benoit a la Guillaume, Phys. Rev. Lett. **45**, 1970 (1980).

[7] I. V. Kukushkin, V. D. Kulakovskii, and V. B. Timofeev, Pis'ma Zh. Éksp. Teor. Fiz. **34**, 36 (1981) [JETP Lett. **34**, 34 (1981)]; V. B. Timofeev, V. D. Kulakovskii, and I. V. Kukushkin, Physica B & C **117-118**, 327 (1983).

[8] J. L. Lin and J. P. Wolfe, Phys. Rev. Lett. **71**, 1222 (1993).

[9] T. Goto, M. Y. Shen, S. Koyama, and T. Yokouchi, Phys. Rev. B **55**, 7609 (1997).

[10] D. W. Snoke, J. P. Wolfe, and A. Mysyrowicz, Phys. Rev. Lett. **64**, 2543 (1990); E. Fortin, S. Fafard, and A. Mysyrowicz, *ibid.* **70**, 3951 (1993); A. Mysyrowicz, E. Benson, and E. Fortin, *ibid.* **77**, 896 (1996); **78**, 3226 (1997).

[11] V. N. Popov, Theor. Math. Phys. **11**, 565 (1972); P. N. Brusov and V. N. Popov, *Superfluidity and Collective Properties of Quantum Liquids* (Nauka, Moscow 1988), Chap. 6.

[12] D. S. Fisher and P. C. Hohenberg, Phys. Rev. B **37**, 4936 (1988).

[13] J. M. Kosterlitz and D. J. Thouless, J. Phys. C **6**, 1181 (1973).

[14] Yu. M. Kagan (unpublished).

[15] W. Ketterle and N. J. van Drutten, Phys. Rev. A **54**, 656 (1996).

[16] S. G. Tikhodeev, Solid State Commun. **72**, 1075 (1989); Zh. Éksp. Teor. Fiz. **97**, 681 (1990) [Sov. Phys. JETP **70**, 380 (1990)].

[17] A. L. Ivanov, C. Ell, and H. Haug, Phys. Rev. E **55**, 6363 (1997).

[18] W. Zhao, P. Stenius, and A. Imamoglu, Phys. Rev. B **56**, 5306 (1997).

[19] I. V. Lerner and Yu. E. Lozovik, Pis'ma Zh. Éksp. Teor. Fiz. **27**, 497 (1978) [JETP Lett. **27**, 467 (1978)]; J. Low Temp. Phys. **38**, 333 (1980); Zh. Éksp. Teor. Fiz. **80**, 1488 (1981) [Sov. Phys. JETP **53**, 763 (1981)].

[20] Y. Kuramoto and C. Horie, Solid State Commun. **25**, 713 (1978).

[21] I. V. Lerner and Yu. E. Lozovik, Zh. Éksp. Teor. Fiz. **78**, 1167 (1978) [Sov. Phys. JETP **51**, 588 (1980)].

[22] For $\nu > 1 T_{cB}(\nu)$ oscillates with minima at integer ν Ref. 19.

[23] L. V. Butov, V. D. Kulakovskii, G. E. W. Bauer, A. Forchel, and G. Grützmacher, Phys. Rev. B **46**, 12 765 (1992).

[24] Yu. E. Lozovik and V. I. Yudson, Pis'ma Zh. Éksp. Teor. Fiz. **22**, 556 (1975) [JETP Lett. **22**, 274 (1975)]; Zh. Éksp. Teor. Fiz. **71**, 738 (1976) [Sov. Phys. JETP **44**, 389 (1976)].

[25] S. I. Shevchenko, Fiz. Nizk. Temp. **2**, 505 (1976) [Sov. J. Low Temp. Phys. **2**, 251 (1976)].

[26] T. Fukuzawa, S. S. Kano, T. K. Gustafson, and T. Ogawa, Surf. Sci. **228**, 482 (1990).

[27] X. Zhu, P. B. Littlewood, M. S. Hybersten, and T. M. Rice, Phys. Rev. Lett. **74**, 1633 (1995).

[28] A. Alexandrou, J. A. Kash, E. E. Mendez, M. Zachau, J. M. Hong, T. Fukuzawa, and Y. Hase, Phys. Rev. B **42**, 9225 (1990).

[29] A. Zrenner, P. Leeb, J. Schäfler, G. Böhm, G. Weimann, J. M. Worlock, L. T. Florez, and J. P. Harbison, Surf. Sci. **263**, 496 (1992); A. Zrenner, in *Festkörperprobleme/Advances in Solid State Physics,* edited by U. Rössler (Vieweg, Braunschweig, 1992), Vol. 32, p. 61.

[30] M. Ma, B. I. Halperin, and P. A. Lee, Phys. Rev. B **34**, 3136 (1986).

[31] M. P. A. Fisher, P. B. Weichman, G. Grinstein, and D. S. Fisher, Phys. Rev. B **40**, 546 (1989).

[32] D. K. K. Lee and J. M. F. Gunn, J. Phys. **2**, 7753 (1990).

[33] W. Krauth, N. Trivedi, and D. Ceperley, Phys. Rev. Lett. **67**, 2307 (1991).

[34] A. Gold, Physica C **190**, 483 (1992).

[35] J. D. Reppy, Physica B & C **126**, 335 (1984).

[36] A. E. White, R. C. Dynes, and J. P. Garno, Phys. Rev. B **33**, 3549 (1986).

[37] R. C. Dynes, A. E. White, J. M. Graybeal, and J. P. Garno, Phys. Rev. B **57**, 2195 (1986).

[38] D. B. Haviland, Y. Liu, and A. M. Goldman, Phys. Rev. Lett. **62**, 2180 (1989).

[39] J. M. Valles, Jr., R. C. Dynes, and J. P. Garno, Phys. Rev. Lett. **69**, 3567 (1992).

[40] D. Yoshioka and A. H. MacDonald, J. Phys. Soc. Jpn. **59**, 4211 (1990).

[41] D. Paquet, T. M. Rice, and K. Ueda, Phys. Rev. B **32**, 5208 (1985).

[42] R. R. Guseinov and L. V. Keldysh, Zh. Éksp. Teor. Fiz. **63**, 2255 (1972) [Sov. Phys. JETP **36**, 1193 (1973)].

[43] Yu. E. Lozovik and V. I. Yudson, Pis'ma Zh. Éksp. Teor. Fiz. **25**, 18 (1977) [JETP Lett. **66**, 355 (1977)].

[44] J. A. Kash, M. Zachau, E. E. Mendez, J. M. Hong, and T. Fukuzawa, Phys. Rev. Lett. **66**, 2247 (1991).

[45] J. E. Golub, K. Kash, J. P. Harbison, and L. T. Floretz, Phys. Rev. B **45**, 9477 (1992).

[46] G. E. W. Bauer, in *Optics of Excitons in Confined Systems*, edited by A. D'Andrea, R. Del Sole, R. Girlanda, and A. Quattropani, IOP Conf. Proc. No. 123, (Institute of Physics and Physical Society, London, 1992), p. 283.

[47] J. Feldmann, G. Peter, E. O. Göbel, P. Dawson, K. Moore, C. Foxon, and R. J. Elliott, Phys. Rev. Lett. **59**, 2337 (1987).

[48] E. Hanamura, Phys. Rev. B **38**, 1228 (1988).

[49] L. C. Andreani, F. Tassone, and F. Bassani, Solid State Commun. **77**, 641 (1991).

[50] B. Deveaud, F. Clerot, N. Roy, K. Satzke, B. Sermage, and D. S. Katzer, Phys. Rev. Lett. **67**, 2355 (1991).

[51] D. S. Citrin, Phys. Rev. B **47**, 3832 (1993).

[52] G. Björk, S. Pau, J. Jacobson, and Y. Yamamoto, Phys. Rev. B **50**, 17 336 (1994).

[53] E. I. Rashba and G. E. Gurgenishvili, Fiz. Tverd. Tela **4**, 1029 (1962) [Sov. Phys. Solid State **4**, 759 (1962)].

[54] D. E. Nikonov and A. Imamoglu (unpublished).

[55] A. B. Dzyubenko and G. E. W. Bauer, Phys. Rev. B **51**, 14 524 (1995).

[56] X. M. Chen and J. J. Quinn, Phys. Rev. Lett. **67**, 895 (1991).

[57] A. Zrenner, J. M. Worlock, L. T. Florez, J. P. Harbison, and S. A. Lyon, Appl. Phys. Lett. **56**, 1763 (1990).

[58] R. Teissier, R. Planel, and F. Mollot, Appl. Phys. Lett. **60**, 2663 (1992).

[59] L. V. Butov, A. Zrenner, G. Böhm, and G. Weimann, J. Phys. IV **3**, 167 (1993); L. V. Butov, A. Zrenner, G. Abstreiter, G. Böhm, and G. Weimann, Phys. Rev. Lett. **73**, 304 (1994).

[60] L. V. Butov and A. I. Filin, Zh. Eksp. Teor. Fiz. (to be published).

[61] G. D. Gilliland, A. Antonelli, D. J. Wolford, K. K. Bajaj, J. Klem, and J. A. Bradley, Phys. Rev. Lett. **71**, 3717 (1993).

[62] V. N. Abakumov, V. I. Perel, and I. N. Yassievich, *Nonradiative Recombination in Semiconductors*, edited by V. M. Agranovich

and A. A. Maradudin (North-Holland, Amsterdam, 1991).

[63] F. Minami, K. Hirata, K. Era, T. Yao, and Y. Masumoto, Phys. Rev. B **36**, 2875 (1987).

[64] M. Maaref, F. F. Charfi, D. Scalbert, C. Benoit a la Guillaume, and R. Planel, Phys. Status Solidi B **170**, 637 (1992).

[65] H. Hilmer, A. Forchel, S. Hansmann, M. Morohashi, E. Lopez, H. P. Meier, and K. Ploog, Phys. Rev. B **39**, 10 901 (1989).

[66] L. V. Butov, A. Zrenner, M. Hagn, G. Abstreiter, G. Böhm, and G. Weimann, Surf. Sci. **361/362**, 243 (1996).

[67] M. Jiang, H. Wang, R. Merlin, D. G. Steel, and M. Cardona, Phys. Rev. B **48**, 15 476 (1993).

[68] B. A. Gergel', R. F. Kazarinov, and R. A. Suris, Zh. Eksp. Teor. Fiz. **54**, 298 (1968).

[69] E. S. Borovitskaya and L. V. Butov (unpublished).

[70] T. Takagahara, Phys. Rev. B **31**, 6552 (1985).

[71] B. L. Altshuler, D. E. Khmel'nitskii, A. L. Larkin, and P. A. Lee, Phys. Rev. B **22**, 5142 (1980).

[72] V. L. Nguen, B. Z. Spivak, and B. I. Shklovskii, Zh. Éksp. Teor. Fiz. **89**, 1770 (1985) [Sov. Phys. JETP **62**, 1021 (1985)].

[73] A. B. Dzyubenko and P. I. Arseev, in *23rd International Conference on the Physics of Semiconductors,* edited by M. Scheffler and R. Zimmermann (World Scientific, Singapore, 1996), p. 2063.

[74] A. E. Bulatov and S. G. Tikhodeev, Phys. Rev. B **46**, 15 058 (1992); S. G. Tikhodeev, Phys. Rev. Lett. **78**, 3225 (1997).

[75] L. V. Butov, in *23rd International Conference on the Physics of Semiconductors* (Ref. 73), p. 1927.

[76] X. Zhang and K. K. Bajaj, Phys. Rev. B **44**, 10 913 (1991).

[77] A. Zrenner, L. V. Butov, M. Hagn, G. Abstreiter, G. Böhm, and G. Weimann, Phys. Rev. Lett. **72**, 3382 (1994).

[78] Yu. E. Lozovik and O. L. Berman, Pis'ma Zh. Éksp. Teor. Fiz. **64**, 526 (1996) [JETP Lett. **64**, 573 (1996)].

[79] B. L. Altshuler, P. A. Lee, and R. A. Webb, *Mesoscopic Phenomena in Solids*, edited by V. M. Agranovich and A. A. Maradudin (North-Holland, Amsterdam, 1991).

[80] P. Dutta and P. M. Horn, Rev. Mod. Phys. **53**, 497 (1981).